AD-A107 677 ROSS ENGINEERING ASSOCIATES INC VALPARAISO FL F/G 1/5
FOD COVER ANALYSIS FOR RAPID RUNWAY REPAIR.(U)
OCT 80 C A ROSS F08635-80-M-0248
UNCLASSIFIED AFESC/ESL-TR-80-59 NL

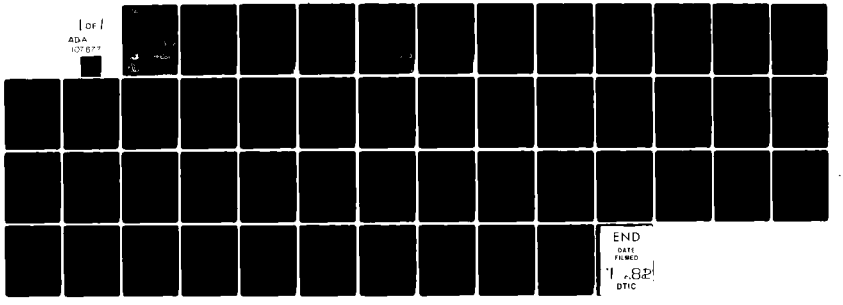

ESL-TR-80-59

2

LEVEL

FOD COVER ANALYSIS FOR RAPID RUNWAY REPAIR

C. A. ROSS

ROSS ENGINEERING ASSOCIATES, INC.
237 S. BAYSHORE DRIVE
VALPARAISO, FLORIDA 32580

30 OCTOBER 1980

FINAL REPORT
30 JUNE 1980 — 30 SEPTEMBER 1980

APPROVED FOR PUBLIC RELEASE: DISTRIBUTION UNLIMITED

AFESC

ENGINEERING & SERVICES LABORATORY
AIR FORCE ENGINEERING & SERVICES CENTER
TYNDALL AIR FORCE BASE, FLORIDA 32403

NOTICE

Please do not request copies of this report from HQ AFESC/RD (Engineering and Services Laboratory). Additional copies may be purchased from:

National Technical Information Service
5285 Port Royal Road
Springfield, Virginia 22161

Federal Government agencies and their contractors registered with Defense Technical Information Center should direct requests for copies of this report to:

Defense Technical Information Center
Cameron Station
Alexandria, Virginia 22314

UNCLASSIFIED

SECURITY CLASSIFICATION OF THIS PAGE (When Data Entered)

REPORT DOCUMENTATION PAGE	READ INSTRUCTIONS BEFORE COMPLETING FORM
1. REPORT NUMBER: ESL-TR-80-59	2. GOVT ACCESSION NO.: AD-A107 677
	3. RECIPIENT'S CATALOG NUMBER
4. TITLE (and Subtitle): FOD COVER ANALYSIS FOR RAPID RUNWAY REPAIR	5. TYPE OF REPORT & PERIOD COVERED: Final, 30 June 1980 - 30 Sept 1980
	6. PERFORMING ORG. REPORT NUMBER
7. AUTHOR(s): C. A. Ross	8. CONTRACT OR GRANT NUMBER(s): F08635-80-M-0248
9. PERFORMING ORGANIZATION NAME AND ADDRESS: Ross Engineering Associates, Inc. 237 S. Bayshore Drive Valparaiso, Florida 32580	10. PROGRAM ELEMENT, PROJECT, TASK AREA & WORK UNIT NUMBERS: PE: 64708F JON: 20546B18
11. CONTROLLING OFFICE NAME AND ADDRESS: Air Force Engineering and Services Center Tyndall Air Force Base, Florida	12. REPORT DATE: 30 October 1980 13. NUMBER OF PAGES: 46
14. MONITORING AGENCY NAME & ADDRESS (if different from Controlling Office)	15. SECURITY CLASS. (of this report): UNCLASSIFIED 15a. DECLASSIFICATION/DOWNGRADING SCHEDULE

16. DISTRIBUTION STATEMENT (of this Report)

Approved for public release: distribution unlimited

17. DISTRIBUTION STATEMENT (of the abstract entered in Block 20, if different from Report)

18. SUPPLEMENTARY NOTES

Availability of this report is specified on verso of front cover.

19. KEY WORDS (Continue on reverse side if necessary and identify by block number)

Rapid Runway Repair
FOD Covers
Plates and Shells

20. ABSTRACT (Continue on reverse side if necessary and identify by block number)

This study is concerned with the response of FOD covers for rapid runway repair. The major portion of the work is in support of the North Field tests. In addition some new repair materials and methods are discussed.

DD FORM 1 JAN 73 1473 EDITION OF 1 NOV 65 IS OBSOLETE

UNCLASSIFIED

SECURITY CLASSIFICATION OF THIS PAGE (When Data Entered)

PREFACE

This report represents the results of a small study in support of foreign object damage (FOD) covers for rapid runway repair. This study was conducted during the period of 30 June 1980 to 30 September 1980, by C. A. Ross of Ross Engineering Associates, Inc., 237 S. Bayshore Drive, Valparaiso, Florida, under Contract No. F08635-80-M-0248, with the Air Force Engineering and Services Center (AFESC), Tyndall AFB, Florida. Mr. P. T. Nash (AFESC/RDCR) served as the project officer for this contract.

This report has been reviewed by the Public Affairs Office and is releasable to the National Technical Information Service (NTIS). At NTIS it will be available to the general public, including foreign nations.

This report has been reviewed and is approved for publication.

Phillip T. Nash
PHILLIP T. NASH
Project Officer

James R. VanOrman
JAMES R. VAN ORMAN
Chief, Rapid Runway Repair Branch

Robert E. Boyer
ROBERT E. BOYER, Lt Col, USAF
Chief, Engineering Research Division

Francis B Crowley III
FRANCIS B. CROWLEY III, Colonel, USAF
Dir, Engineering and Services Laboratory

Accession For	
NTIS GRA&I	X
DTIC TAB	☐
Unannounced	☐
Justification	
By	
Distribution/	
Availability Codes	
Dist	Avail and/or Special
A	

(The reverse of this page is blank)

TABLE OF CONTENTS

LIST OF FIGURES

LIST OF FIGURES (CONTINUED)

LIST OF TABLES

SECTION I

INTRODUCTION

Runway damage in general comes in many forms and is classified and discussed in many publications too numerous to be included here. The same may be said of the repair of damaged runways and no attempt will be made here to review the historical background of methods of runway damage or repair.

Runway damage as defined in this report means that a portion of the runway, 10 to 20 feet (approximately 3-6 m) in diameter, has been damaged by some method and the entire damaged area, including portions of the sub-base, must be removed and replaced by suitable repair materials and methods. However, the repair, temporary in nature, must be done as quickly as possible and in such a fashion as to allow aircraft takeoff and landings.

This report covers two small portions of the overall runway damage and rapid runway repair area. The two main phases, as specified in the contract, to be addressed were (I) develop analytical techniques to evaluate thin flexible covers, available in the Air Force inventory, to be used to prevent foreign object damage (FOD) from a damaged crater filled with crushed limestone and (II) recommend other methods of repair and present design curves for same. Phase I was considered the most immediate requirement and was to be accomplished to support the North Field tests where repair materials were already specified. The Phase II was to be accomplished as time permitted under the contract period.

The remainder of the report will be broken into two parts covering both Phase I and Phase II respectively.

SECTION II

PHASE I

1. MATERIAL PROPERTIES TESTS

a. As-Received Material

The main material in question to be used in Phase I was a flexible cover known as T17 (Reference 1). Some of the properties of the material are given in Reference 1, however, for an analysis a stress strain curve or constitutive relation is required. In order to establish this data, a series of tests were conducted to determine both a stress-strain curve and ultimate strength of the T17 material. The stress-strain curve, obtained experimentally, and shown in Figure 1, was used in all analyses to be discussed in the following sections. The breaking strength of 420 lb/in (736 nt/cm) is slightly higher than the value of 365 lb/in(639 nt/cm) reported in Reference 1.

The stress-strain curve was determined by measuring the elongation of a 50 mm long gage length in the middle of a 127 mm reduced cross section specimen. The material behaved nonlinear elastic as shown in Figure 1. After removal of the loads, up to approximately 12 percent strain, the material returned to its original length with resulting permanent strains of less than 1 percent.

b. High Temperature Test

The temperature effects resulting from jet blast on the cover material were investigated by applying heat by open flame from a small propane torch to test specimens both before and during loading. Prior to testing the tensile samples, pieces of the material with a thermocouple imbedded in them were subjected to the open flame. It was determined that the temperatures of approximately 300°F (149°C) could be reached without actual burning or charring the material. (Prolonged application of the flame above this temperature resulted in flaming of the material after removal of the torch.)

These tensile specimens (1.0 inch (2.54 cm) wide at test section) were heated to approximately 300°F (149°C) then cooled and tested at room temperature. The results of these three tests showed very similar results to those of the as-received material reported on previously. Elongation appeared to be similar and fracture occurred at a point outside the heated area.

Two as-received specimens were placed in the tensile machine and loaded to 200 lb/in (350 nt/cm). The specimens

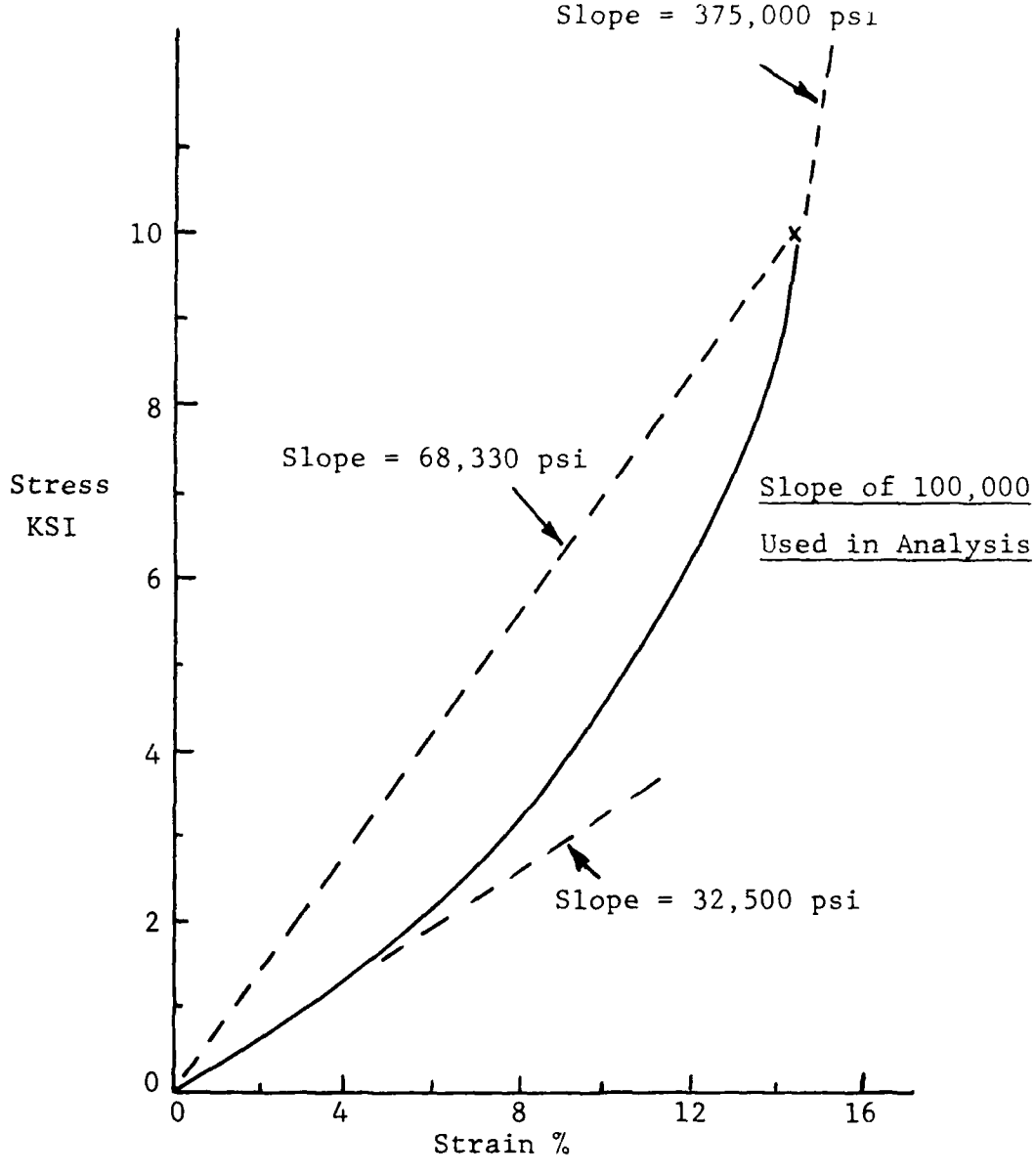

Figure 1. Stress-Strain Curve T17 FOD Cover Material.

were then heated under load to approximately 300°F (149°C). An immediate drop in the load to approximately 150 lb/in (263 nt/cm) was experienced. This indicates that elongation has occurred due to change in temperature. Continued loading of the heated specimen resulted in an average breaking strength of approximately 200 lb/in (438 nt/cm). Elongation of the heated specimen was not measured but it appeared to be about the same or slightly greater than the as-received specimen elongation. However, for the heated specimens under load, the fracture occurred in the heated area.

Based on these limited tests it appears that local one-cycle heating, that does not actually burn the fibers or coating, and subsequent loading does not have much effect on the mechanical properties of the material. However, simultaneous heating and loading does show reduction in the fracture strength of the cover material. These statements must be restricted to one-cycle heatings/loadings and would not necessarily apply under repeated loadings and/or heatings.

c. Post Service Tests

A portion of the T17 FOD cover, which had been used in over fifty F-4 and C-130 operations of the North Field Test, was cut into 8.0 x 1.5 inch (20.32 x 3.81 cm) test specimens and loaded until failure. Same size specimens of the "as received" material were also tested at the same time. Five specimens of each were tested and the average failure load of each was determined. The ratio of the average failure load of the post service test specimens to that of the as-received test specimens was found to be 0.576.

The failure of the post service test specimen appeared to always occur at a small tear on the underside of the material which had been exposed to the crushed limestone.

2. MEMBRANE ANALYSIS

a. Preliminary Analysis

In the repair procedure, the damaged area is cleared of debris and the crater filled with crushed limestone then compacted and graded. The final step is to cover the graded limestone with a flexible membrane (T17) to prevent foreign object damage (FOD) during aircraft operations. A major concern was the response of this membrane covering (hereafter referred to as the FOD cover) to aircraft weight and loadings caused by braking and jet blast.

Aircraft loadings exerted on the repaired surface are complicated by the motion of the aircraft but the major normal loads

(perpendicular to runway) and braking loads in the plane of the runway decrease as the aircraft velocity and lift forces increase. This means that at taxi velocities the normal and braking loads are at their maximum. In the analyses that follow it is assumed that the dynamic or inertia loads are negligible. It may be that the inertia loads are very important at high velocity passes across a repaired area but that aspect of the study was considered beyond the scope of this report.

For the membrane analysis, the braking loads are the primary concern and for the flexible FOD cover the bending loads caused by the weight of the aircraft are negligible. In later discussions for thick coverings the bending loads must be considered.

In an initial effort to examine the response of the FOD cover to the braking load of an aircraft, a membrane finite element analysis was employed. The membrane element is one of the standard elements of the computer code SAPIV (Reference 2). Shown schematically in Figure 2, a 6 x 6-foot (1.83 m x 1.83 m) FOD cover was broken into 6-inch (15.24 cm) square elements, loaded on one free edge and bolted on the opposite edge with the other two edges free. This model stems from the 12 x 6-foot (3.66 m x 1.83 m) panel of the F-4 braking tests of July 8, 1980, Tyndall Air Force Base. Since the FOD cover can only carry a very minimal inplane compressive load, only the membrane between the load and the bolted edge were used in the model.

The load is applied as 100 pounds (445 nt) scattered in four 10-pound (44.5 nt) load points surrounding a 60-pound (267 nt) point shown at the nodes 137, 149, 150, 151, and 163 of Figure 2. The objective of this study is to show that as more and more hold-down points are fixed the stress at the individual pins is reduced while the stress near the load remains nearly the same for each pinned edge case. The analyses were accomplished using this constant load distributed as previously described for a combination of pins on the resisting edge as given in Table 1.

TABLE 1. RESISTING NODE COMBINATIONS

Case	Number of Nodes Pinned	Pinned Node Nos.
A	2	1, 13
B	3	1, 7, 13
C	5	1, 4, 7, 10, 13
D	12 (entire edge)	1, 2, 3, 4, 5, 6, 7, 8, 9, 10, 11, 12, 13

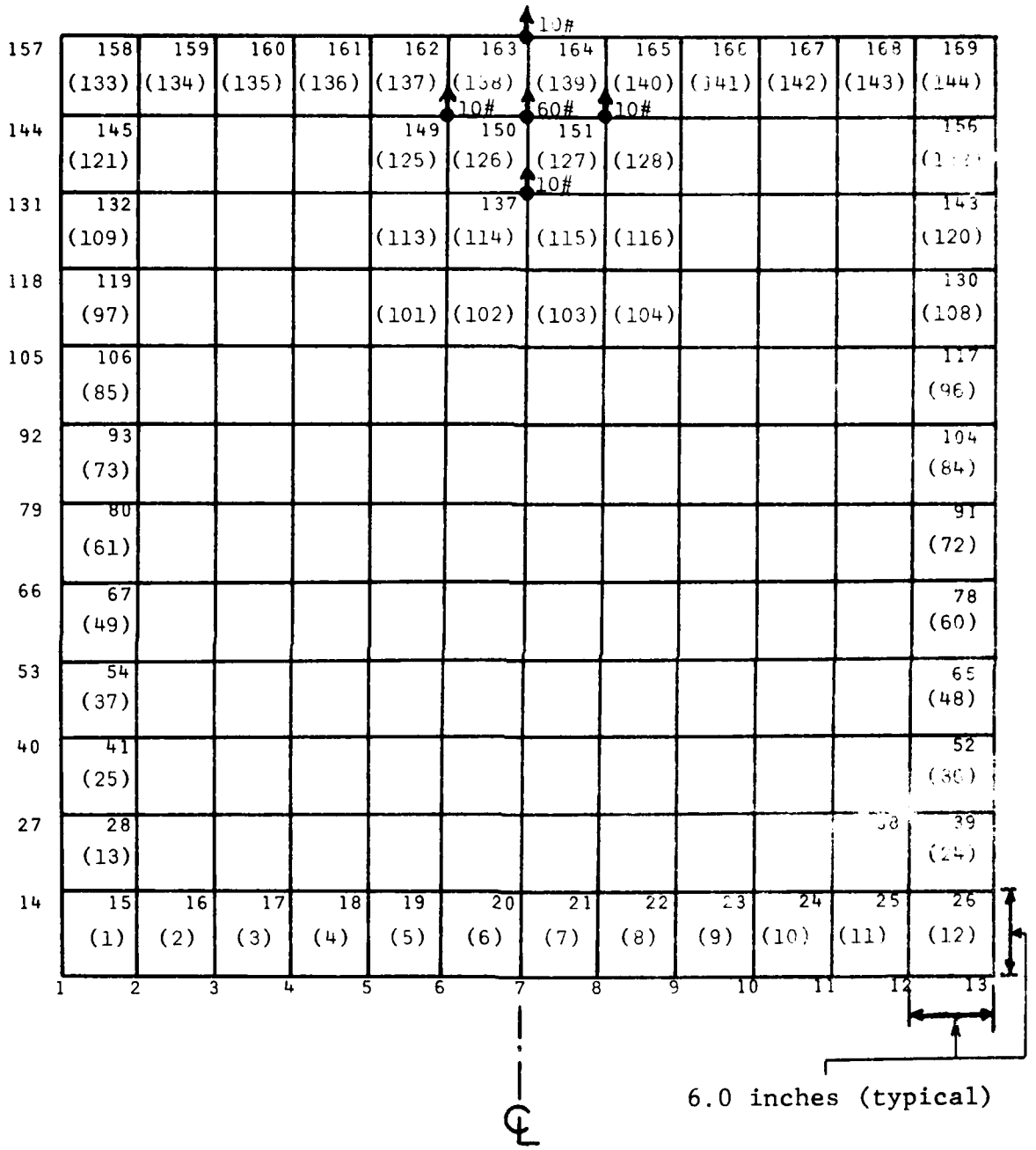

Figure 2. Nodes and Elements Used in the Preliminary Finite Element Analysis of the T17 FOD Cover. Node Numbers are Given Just to the Lower Left of the Nodes and Element Numbers are Given in the Middle of the Elements. The Load is Shown to the Right of the Arrows With A # Symbol.

The stress distributions for the given resisting node combination are shown in Figures 3 through 6. The stress distributions show the tensile principal stress and its direction. The maximum principal stresses and their direction are shown in the elements of the membrane with stress shown on top and the angle given beneath the stress value. The loading is shown at the top of membrane and the pins are shown as circled nodes at the bottom of each figure. Due to symmetry of the problem only half of the membrane is shown for each of the Figures 3 through 6. The angle is measured from a horizontal line parallel to the bottom row of pins. It is worthy to note the gradual reduction in stress at the pins as the number of pins is increased, while the stress at the loadings remains almost constant.

In addition a series of small plastic sheets were tested as shown in Figure 7. The plastic sheet was much thinner and weaker than the T17 FOD cover material, but nevertheless acts as a membrane and displays the same characteristics as shown in real test and the above analyses. The tests were performed on a full panel and loaded inplane at the center as shown in Figure 7. The load was not measured, but each time the load was increased until a point in the sheet ruptured. The resisting edge pin combinations used in the test are given in Table 2.

TABLE 2. THIN PLASTIC RESISTING PIN COMBINATIONS

Case	Pins Used (Equally Spaced)
1	2
2	3
3	5
4	7
5	Whole edge fixed

The thin plastic sheet showed similar results as discussed in the Analyses. For the two-pin case, rupture of the sheet occurred at one of the pins. For the three-pin case, both pin and load points showed considerable deformations and it appeared that material at a pin and at load failed almost simultaneously. For the five-pin case, the material at the loading point failed with very little deformation at the pins. For the case of the sheet sandwiched between two plates, very little deformation occurred at any of the fixed edges because failure occurred under load.

b. Full Scale Analysis

Based on the preliminary analysis of the FOD cover and the simple thin plastic sheet tests, it was agreed that a minimum of

	1 -65		5 52	35 40	87 28						
1 -19	3 -9	12 35	31 41	69 51	139 68						
1 13	10 48	24 48	45 52	74 61	103 78						
5 50	19 57	33 56	49 60	64 69	73 82						
12 67	26 62	38 61	48 64	54 72	57 83						
21 75	33 65	42 63	46 64	46 71	45 82						
33 78	41 66	45 62	44 62	39 66	34 80						
47 80	51 66	49 59	43 56	34 57	25 71						
66 80	63 64	54 54	41 48	28 47	18 51						
94 78	79 60	57 45	33 39	20 38	12 31						
143 75	103 46	34 30	18 34	8 38	4 51						
272 60	18 9	7 66									

Figure 3. Stress Distribution for Pins at Two Points. Pins Shown as Circled Nodes. Stress is Given as Top Number and Angle Given as Lower Number. Positive Angle Measured CCW from Horizontal. Stress in PSI and Angle in Degrees.

	1 -64	1 -80	4 62	33 42	84 29						
1 -21	3 -31	10 36	28 43	67 53	139 68						
1 2	7 48	21 51	41 55	73 64	104 79						
2 34	14 59	28 60	45 65	64 72	76 84						
6 61	19 65	32 67	45 71	56 78	62 86						
11 74	23 70	33 71	42 75	49 80	53 87						
17 79	26 72	33 73	39 77	44 83	47 88						
24 81	30 72	33 73	36 79	40 85	44 89						
33 80	34 68	31 67	30 81	37 -88	44 -89						
47 78	41 60	29 48	21 -74	37 -75	49 -85						
73 74	52 46	18 28	12 -12	46 -52	69 -78						
136 61	4 12	3 77	3 -90		132 -61						

Figure 4. Stress Distribution for Pins at Three Points. Pins Shown as Circled Nodes. Stress Given as Top Number and Angle Given as Lower Number. Positive Angle Measured CCW from Horizontal. Stress in PSI and Angle in Degrees.

	1 -64		4 60	34 41	85 29						
1 -21	3 -28	10 36	28 43	67 53	139 68						
1 4	8 48	21 57	41 55	72 64	104 79						
2 38	14 59	28 60	45 65	64 73	76 84						
6 63	19 65	31 67	44 71	55 78	62 86						
11 75	22 70	33 72	42 76	48 81	53 87						
17 81	25 75	33 76	40 78	45 82	47 87						
21 84	27 79	33 78	38 80	41 83	43 88						
25 86	30 80	34 79	36 81	38 84	39 88						
29 85	32 79	33 78	35 82	36 85	36 87						
40 74	30 63	34 -86	38 75	31 80	37 -82						
74 62	1 9	61 -66	68 62	-2 18	65 -65						

Figure 5. Stress Distribution for Pins at Five Points. Pins Shown as Circled Nodes. Stress Given as Top Number and Angle Given as Lower Number. Positive Angle Measured CCW from Horizontal. Stress in PSI and Angle in Degrees.

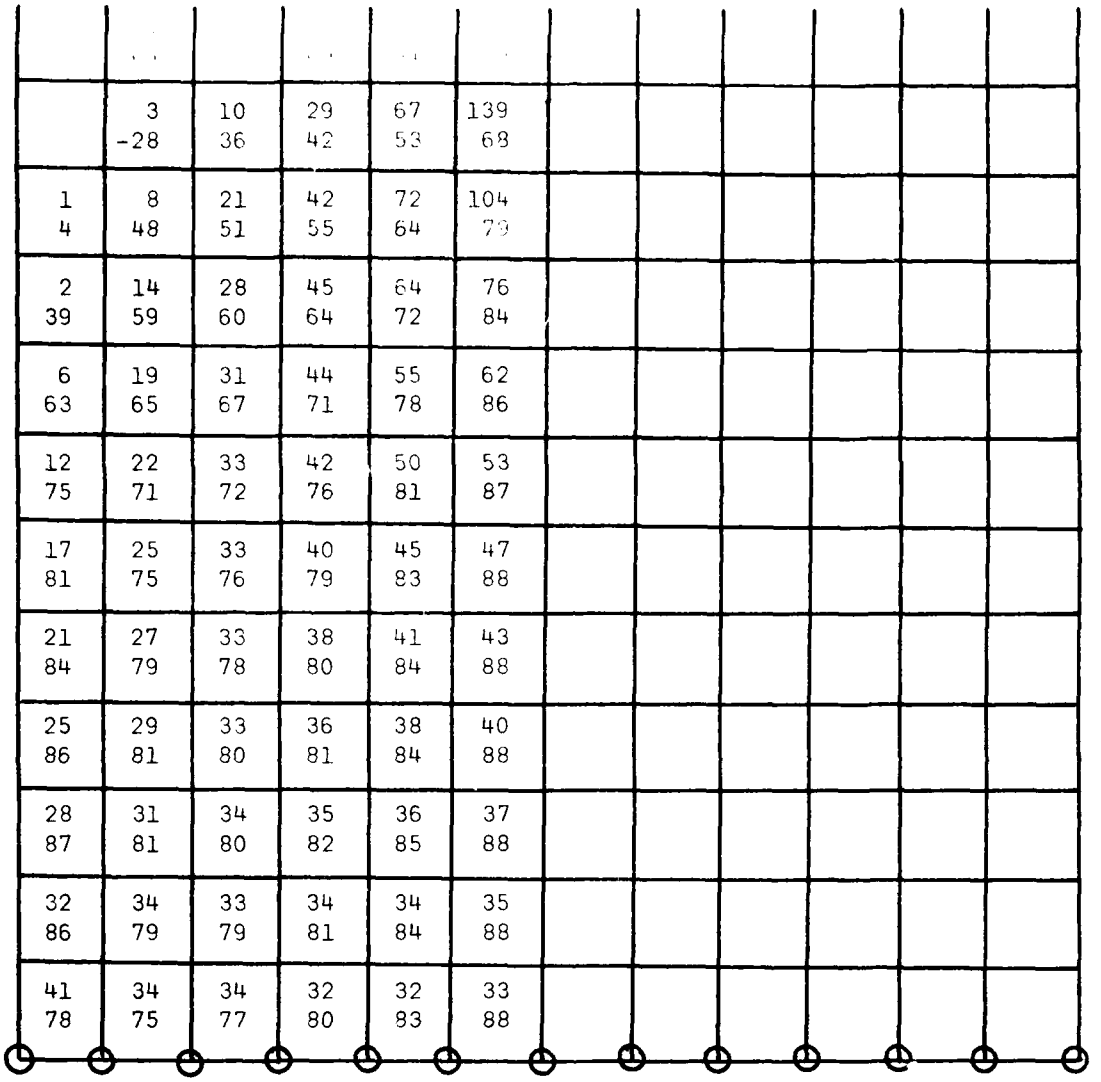

Figure 6. Stress Distribution for Pins at All Nodes of Bottom Edge. Pins Shown as Circled Nodes. Stress Given as Upper Number and Angle Given as Lower Number. Positive Angle Measured CCW from Horizontal. Stress in PSI and Angle in Degrees.

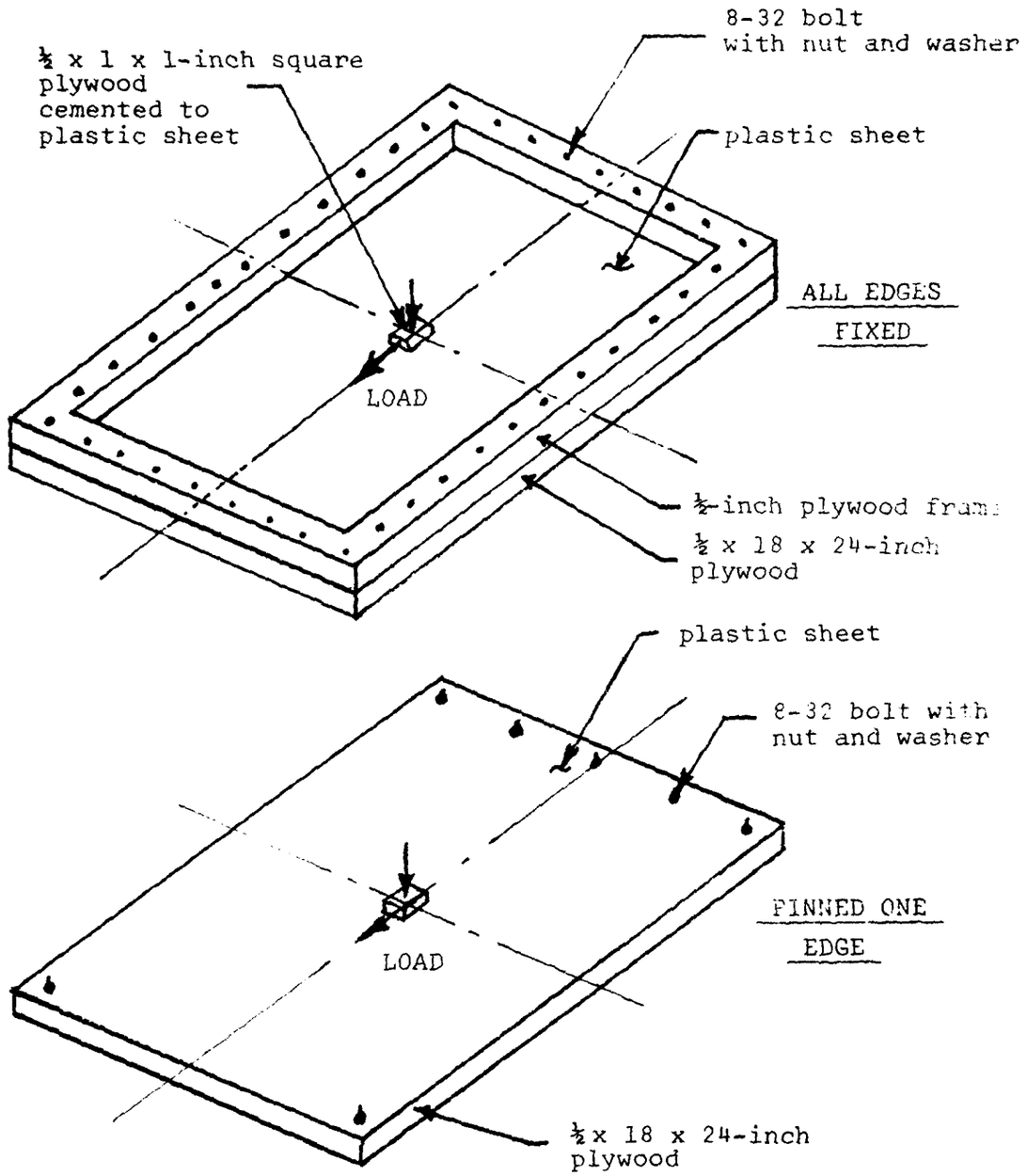

Figure 7. Schematic of Loading Frames for Simple Test on Thin Plastic Sheet.

six-pinned positions is sufficient to give an almost uniform edge load and also insure that failure would occur at the membrane center positioned applied load and not at the pinned edge. The main advantage for failure occurring at a point away from the pins is that repair by contact cementing is much easier and faster if the hold down pins and bars do not have to be removed, as would be the case if failure at the pins occurred.

Using seven pinned positions, a 30-foot (9.15 m) square FOD cover was analyzed using the same SAPIV Code as before. The element size in this case was 1.0 foot (0.30 m) square except the element size around the loading was reduced to 0.5 foot (0.15 m). The same 100-pound (445 nt) load was applied at the center of the FOD cover and stress distribution determined for the 0.042-inch (0.11 cm) thick material with an assumed modulus of 1.0×10^5 psi. The FOD cover was assumed pinned every 5.0 feet (1.52 m) or at a total of seven places behind the load and the sheet forward of the load was neglected.

The stress distribution as shown in Figure 8 is very similar to that of the five-pinned cover of Figure 5. The stress distribution indicates that as the loading is increased the failure would tend to occur under the load, if the basic assumptions are correct.

If the failure stress is approximately 10,000 psi (68.94 MPa) as given in Figure 1, then the maximum braking load (load in the plane of the membrane), assuming no stress concentrations, may be calculated using the maximum stress for the 100-pound (444.8 nt) load. This results in (10,000/181) x 100 = 5525 pounds (24.57 knt) for the maximum braking load. However, a stress concentration factor of at least two might be expected which reduces the maximum braking load for the T17 FOD cover to approximately 2800 pounds (12.29 knt). This is considerably less than the maximum braking load of 10,240 pounds (45.55 knt) as reported for a heavy F-4 aircraft. This confirms analytically that braking should be avoided on the T17 FOD cover by F-4 aircraft.

If the T17 material thickness could be increased during fabrication and assuming the strength to be linear with increased thickness, a design curve may be constructed for the heavy F-4 aircraft. This curve is shown in Figure 9. Any conclusions drawn from these curves must not imply the use of several layers of the current T17 material.

At the pins or bolts of Figure 8, the stress appears to be about 1/6 of that at the load position. Using a stress concentration of three at the pins still indicates that failure would occur first in the cover under the applied braking load, which has been confirmed by the taxi test at Tyndall Air Force Base and thin plastic sheet specimens discussed previously. It must be pointed

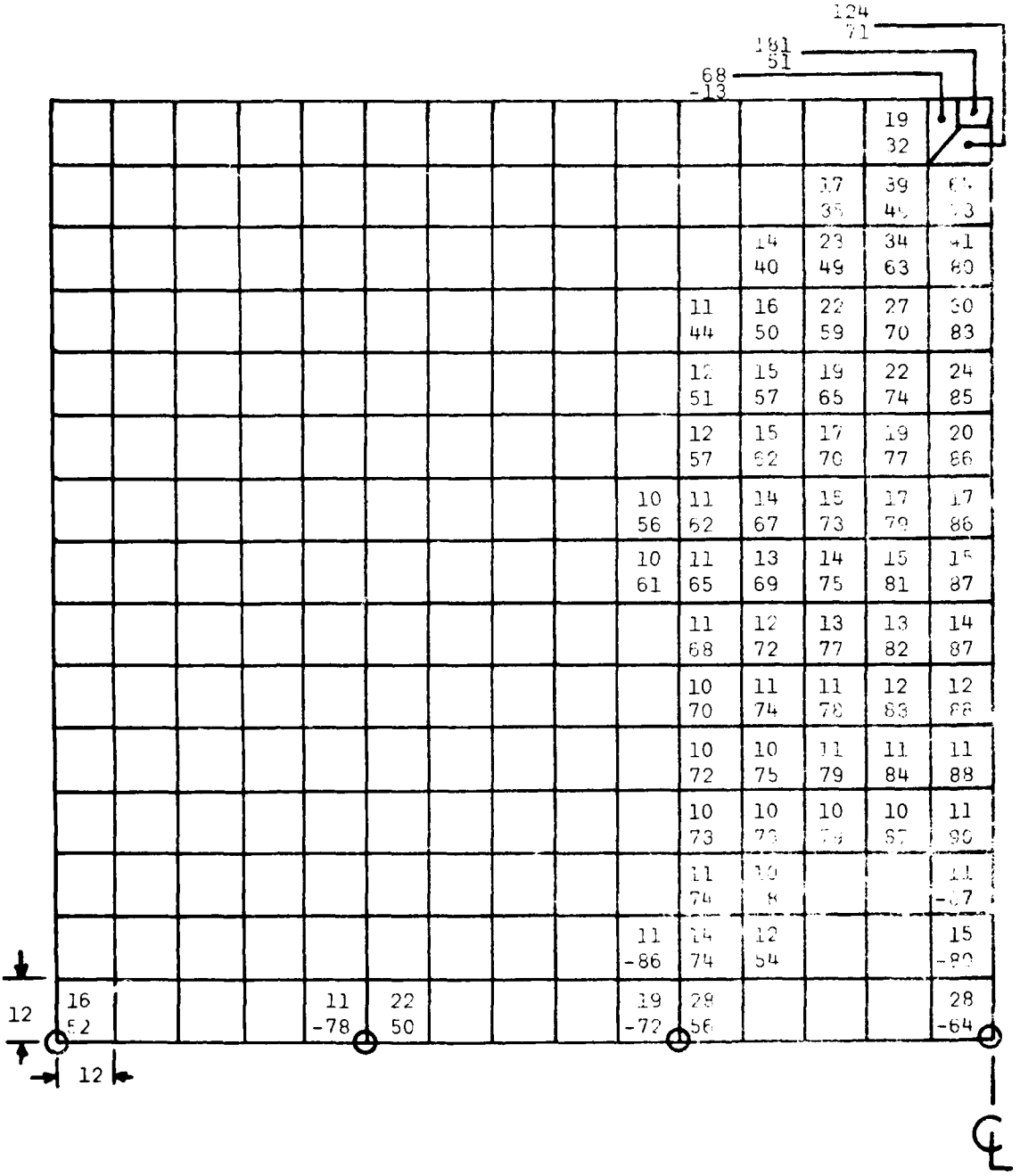

Figure 8. Full Scale FOD Cover Analysis. FOD Cover Size 30 x 30 Feet (9.15 x 9.15 m) Pinned at Seven Places as Shown by Circles at Lower Nodes. Total Load of 100 Pounds (445 nt) Distributed at Center of Cover as Shown in Figure 2. All Stresses Less Than 10 psi are Omitted. T17 Material 0.042-inch (0.11 cm) Thick. Stress in PSI and Angle in Degrees.

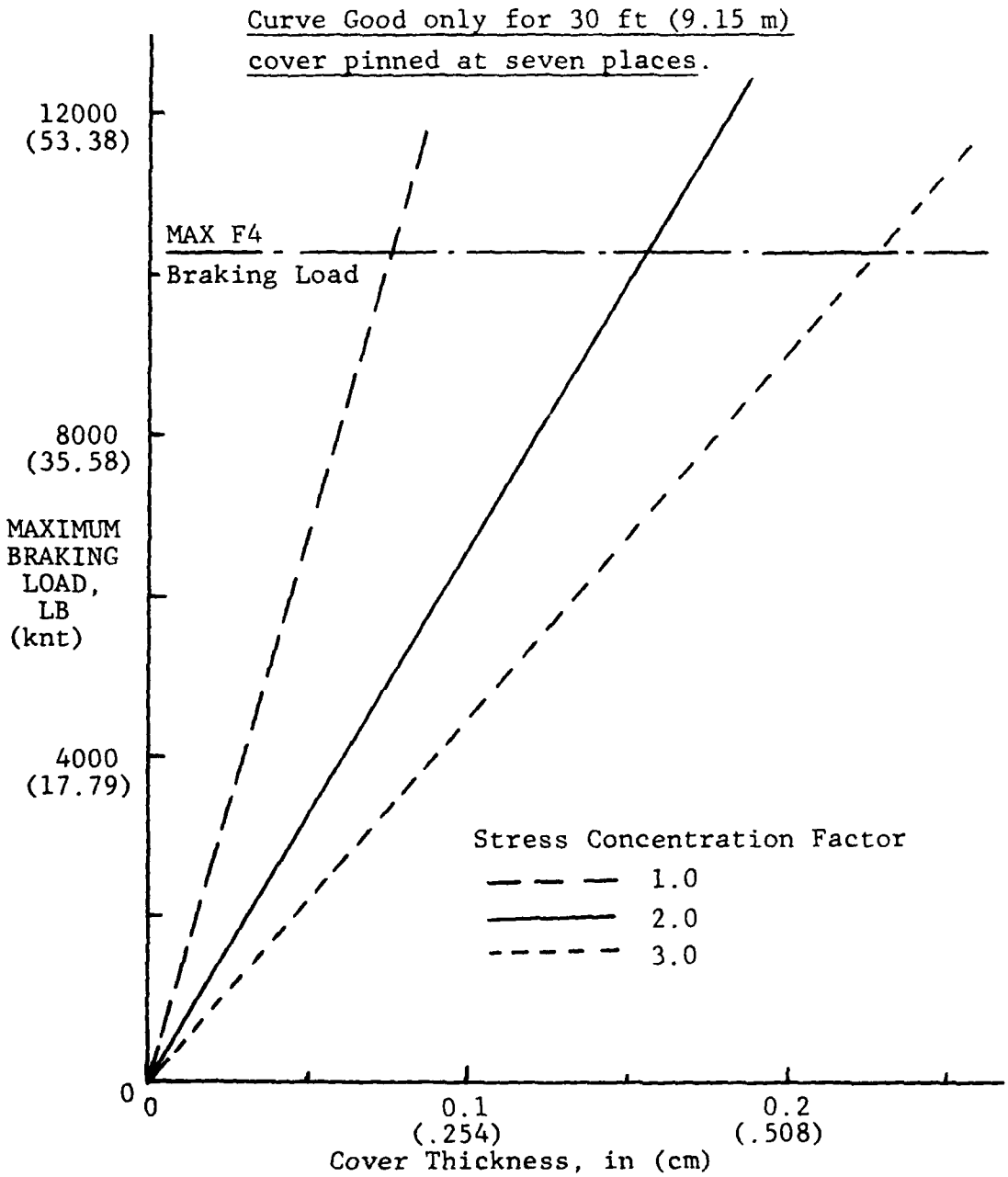

Figure 9. Maximum F-4 Braking Load for Given Thickness of Material Similar to T17.

out that the above discussion is based on the 30-foot (9.15 m) square FOD cover and changes in size could change the results of the analysis.

c. Jet Blast Analyses

The main objectives of this portion of the FOD cover analyses are to explore the advantages gained by fixing the sides of the cover and discuss lift or vertical forces due to the jet blast.

A full scale jet blast test on an FOD cover was conducted by use of an F-4 aircraft at Tyndall Air Force Base, Florida. These tests indicated that jet blast flowing over an FOD cover could cause considerable damage if the blast was allowed to get under the FOD cover. If the blast or atmospheric pressure is allowed under the cover, considerable billowing of the cover occurs and failure may occur due to increased tension in the cover coupled with the strength reduction due to temperature effects. The billowing or lift of the cover could possibly be prevented or reduced by pinning all four edges of the cover.

The comparison of fixed cover sides to free cover sides is made on the basis of cover center point displacement of an elastic, uniformly loaded plate and membrane. The major difference between a plate and a membrane is the assumption as to how the load is distributed in the plate or membrane material. For the plate, the assumption is that the load is resisted as bending of the plate with no midplane loading. On the other hand the membrane is assumed to resist displacement through its initial midplane tension.

The expressions for out of plane center point displacement of the plate were taken from Reference 2 and are given in Table 3. The expressions for out of plane displacement of the membrane were derived based on methods given in Reference 3 and are also in Table 3.

For the plate, the ratio of center point displacement for free sides to fixed sides is about 3.22. However, the same ratio for membranes is only 1.39. It is important to note that these comparisons are for elastic, small displacements in plates and membranes. For large displacements the ratios may not be as large, but are expected to be greater than 1.0.

In an effort to determine lift forces on the membrane resulting from the jet blast the following procedure or analysis was adopted. Based on T.O. 1F-4E-2-1 jet velocities of 800 ft/s (244 m/s) may be experienced as far back as 15 feet (4.57 m) from the rear nozzle of a single afterburner. Using the properties of standard air the dynamic pressure ($0.5\ \rho V^2$, where ρ = density and V = velocity) is approximately 5.28 psi (36.4 kPa) for this

TABLE 3

OUT OF PLANE DISPLACEMENTS FOR UNIFORMLY LOADED PLATES AND MEMBRANES

Boundary Conditions	Center Point Displacement
PLATES	
Two sides clamped Two sides simply supported	$0.00192qa^4/D$
All edges clamped	$0.00126qa^4/D$
All edges simply supported	$0.00406qa^4/D$
Two edges simply supported Two edges free	$0.01309qa^4/D$
MEMBRANES	
All edges simply supported	$0.0965qa^2/\sigma h$
Two edges simply supported Two edges free	$0.134qa^2/\sigma h$

a = width
h = thickness
ν = Poisson's ratio
q = uniform load

E = modulus of elasticity
$D = Eh^3/12(1-\nu^2)$
σ = membrane stress
σh = membrane force/unit length

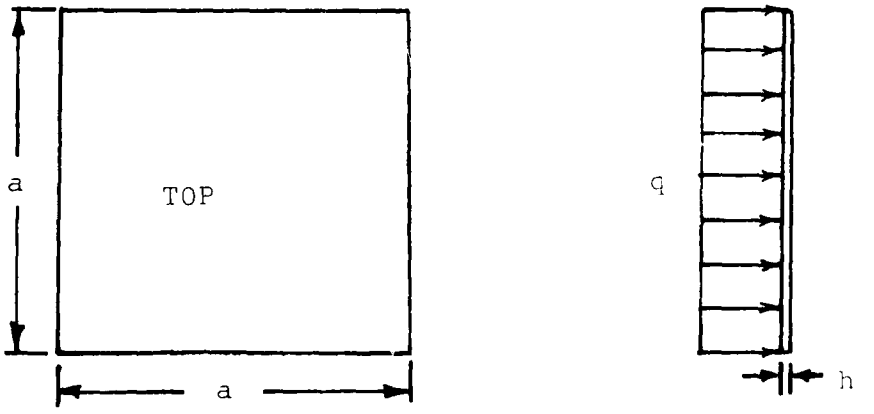

velocity and acts at an angle of 7-10 degrees from the plane of the membrane. The inplane force generated in the cover is assumed to be sufficient to push all the slack in the cover rearward causing buckling and humps in the cover. These humps are then exposed to dynamic pressure which further stretches the cover causing a larger hump to form. This hump now gives rise to lift or vertical forces which aggravate the condition and cause the hump to increase in height, etc.

The vertical or lift force may be estimated assuming the hump that is formed is a half cylinder with its longitudinal axis normal to the jet velocity vector. Using Figure 10 and a uniform freestream velocity U_0, the velocity vector V, for potential flow, at the surface of the cylinder is given in Reference 4 as

$$V^2 = 4U_0{}^2\sin^2\theta \quad . \tag{1}$$

Using Bernoulli's equation,

$$0.5\rho V^2+p = \text{constant} = C \quad , \tag{2}$$

where ρ is density, p is the local static pressure, $C = p_0+0.5\rho U_0{}^2$ from stagnation conditions, and p_0 is the free stream static pressure. The normal pressure acting on the upper surface of the half cylinder then becomes

$$p = p_0+\rho U_0{}^2(0.5-2\sin^2\theta) \quad . \tag{3}$$

Assuming the pressure underneath the half cylinder and cover to be equal to the free stream static pressure and for flow open to the atmosphere this then becomes atmospheric pressure. Integrating the pressure p over the upper surface of the half cylinder and p_0 over the diameter of the lower surface (Figure 9) the vertical force per unit length of the half cylinder of radius b becomes

$$F_V = 1.667b\rho U_0{}^2 \text{ lb/in} \quad . \tag{4}$$

Using equation (4), U_0 = 800 fps, and ρ = 0.002378 slugs/ft^3 the force F_V becomes 17.62b lb/in.

Now the question becomes will the membrane fail under the conditions of an 800 ft/s (244 m/sec) free stream jet blast. A 1.0 to 2.0 psi (6.89-13.78 kPa) uniform inplane stress on a 30-foot (9.15 m) long cover is sufficient to cause a 10 percent elongation of the membrane and cause a hump to form near the end of the cover. Assuming all the 10 percent elongation (36 inches for a 30-foot long strip) goes to form a cylindrical hump, results in a radius b = 11.46 inches (29.11 cm). From the previous calculations of F_V = 17.62b and using b = 11.46 inches (29.11 cm) the vertical force per unit half cylinder length becomes 202 lb/in (354 nt/cm). This running load is resisted by the membrane at two

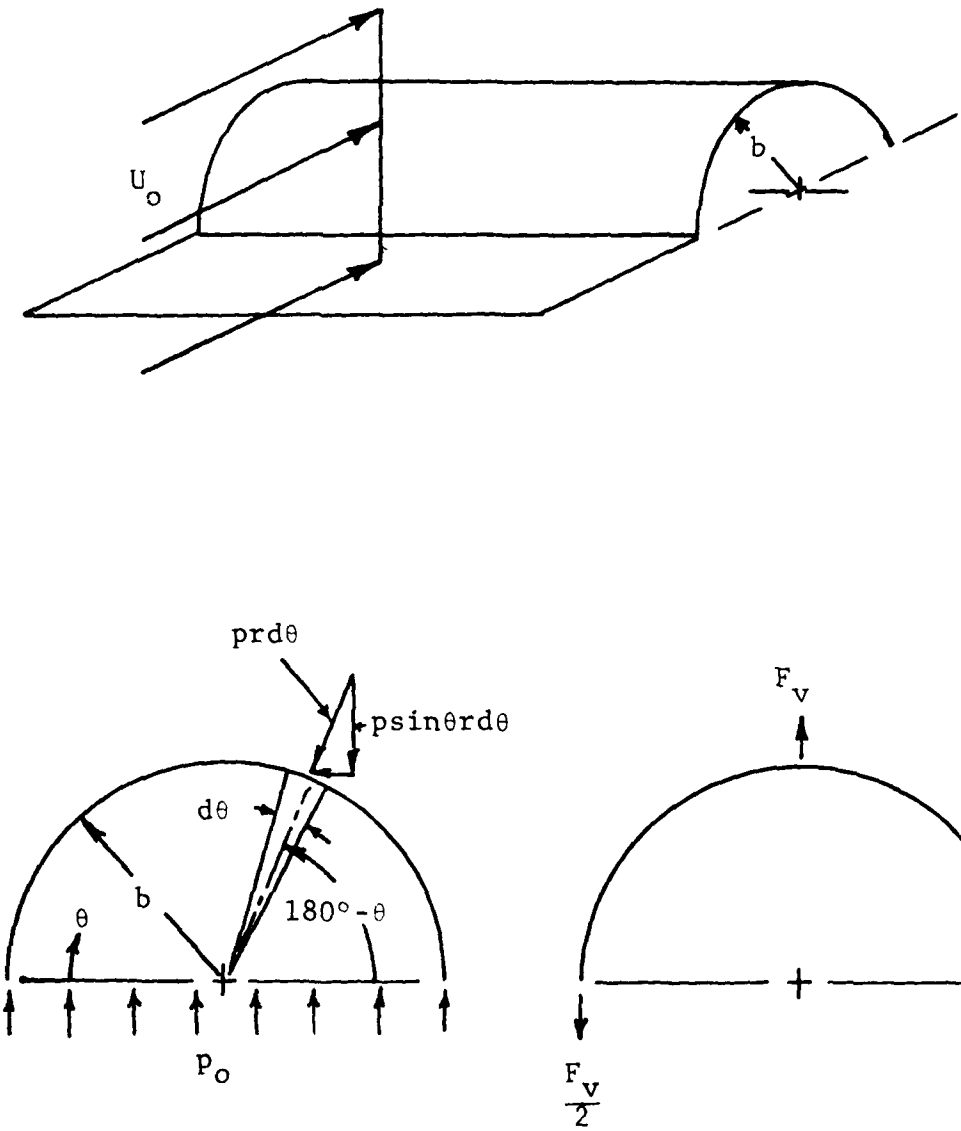

Figure 10. Flow Over a Half Cylinder.

points (Figure 8) which results in a stress of approximately 100 lb/in (222 nt/cm) that now must be carried by the membrane in addition to the load causing the initial stretching which at 10 percent strain is approximately 200 lb/in (444 nt/cm). The rupture strength of the FOD cover material (T17) was found to be 400-420 lb/in (700-736 nt/cm) by test as given previously in Figure 1. However, at elevated temperature of 300°F (149°C), the rupture strength may be as low as 200 lb/in (444 nt/cm) and would result in failure of the FOD cover under steady state blast conditions.

3. PHASE I DISCUSSION, CONCLUSIONS AND RECOMMENDATIONS

Results of both tests and analyses show that braking on the T17 material of 0.042-inch (0.107 cm) thickness should be avoided. However, failure due to braking inplane loads will occur at the centered load point rather than at the pinned sides.

Based on the full scale elastic analysis with pinned edges every 5 feet (1.52 m), the maximum load on the middle bolt or pin is about 25 percent of the braking load. For the T17 0.042-inch (0.107 cm) thick material, the maximum braking load without stress concentration is approximately 5600 pounds (24.9 knt). For this analysis the maximum load on one bolt would be about 1400 pounds (6.23 knt). For increased cover thickness and a reduction of the number of pins or bolts this load would increase. For other size covers and pin combinations, separate analyses would be accomplished. Because of time limitations on the contract period these additional analyses could not be accomplished at this time.

Due to loss of strength at elevated temperatures and increased loading caused by lift forces, jet blast on the FOD cover for more than 2 to 3 seconds should be avoided. In addition, jet blast directed transverse to the free edge should be avoided completely. A method for reducing the probability of introducing the jet blast under the FOD cover on the runway is to increase the width of the cover transverse to the direction of the runway. Increased width of the cover may alleviate problems associated with the localized jet blast of small aircraft but will not be sufficient for the "prop wash," wing vortex action, and extensive jet blast of larger aircraft. Pinning of all four sides of the FOD cover could almost eliminate the lifting of the cover due to jet blast, however this would increase the repair time. Further discussions of this will be given in Phase II.

SECTION III

PHASE II

1. INTRODUCTION

As discussed previously, the preceeding Section I is concerned with analysis of a specific FOD cover material, namely, the T17 material. This portion of the report is concerned with other kinds of material and methods for rapid runway repair. The major portion of the contract was devoted to Phase I and time limitation prevented putting much emphasis on Phase II. However, some other materials and analyses were considered and the results are presented in the following sections.

If the cover material gets reasonably thick, then bending stresses become important and must be taken into account. For elastic analyses the bending and membrane loads may be treated separately. Membrane stresses are developed in plates with transverse loadings but for small deflections and thick plates these membrane stresses are almost negligible. In the following analyses, only bending stresses will be assumed to be developed by transverse loads and only membrane stresses will be assumed to be developed by inplane loadings.

The analyses of plates for use as FOD covers are further complicated by the resisting forces of the foundation on which the plate is placed. A general procedure is to assume the foundation exerts a force linearly proportional to the transverse deflection of the plate. This subject is usually lodged under the general subject of plates on elastic foundations and is covered in some detail in References 2 and 3. Closed form infinite series solutions for the deflections and resulting bending stresses of a simply supported (all four edges) plate on an elastic foundation are given in Reference 3 for various loadings. The loading which best represents an aircraft tire and wheel is the solution of a small loaded area on the plate, however, in the analysis if the loaded area is small compared to the overall plate area the convergence of the series solution is very slow. For this study a small loaded area with a uniform load equal to the aircraft tire pressure will be used with regular plate theory. Particular attention will be given to insure convergence of the series solution in the range of thicknesses used. In general the regular plate theory neglects midplane stretching, assumes small deflections, neglects stresses normal to the plate, assumes plane sections remain plane, assumes small thickness to lateral dimensions ratio and a linear elastic constitutive relation.

For a plate on an elastic foundation with a fixed load, the maximum bending stress occurs at the plate center and when the

load is applied at the plate center. For rectangular plates this maximum stress is in a direction perpendicular to the long side of the plate. Based on the above, the maximum bending stress of a plate simply supported by an elastic foundation and shown schematically in Figure 11 is given by

$$\sigma_{max} = \frac{96a^2}{h^2} p_0 \sum_{m=1}^{\infty} \sum_{n=1}^{\infty} \frac{\left[\nu m^2 + \left(\frac{a}{b}\right)^2 n^2\right] \left[\sin\frac{m\pi c}{2a} \sin\frac{n\pi d}{2a}\left(\frac{a}{b}\right)\right]}{mn\left\{\pi^4\left[m^2+\left(\frac{a}{b}\right)^2 n^2\right]^2 + \frac{a^4 k}{D}\right\}} \qquad (5)$$

$$m = 1,3,5,\ldots,$$
$$n = 1,3,5,\ldots,$$

where

σ_{max}	= maximum bending stress	psi(Pa)	,
a	= long length of plate	in(m)	,
b	= short length of plate	in(m)	,
c,d	= loaded area dimensions	in(m)	,
h	= plate thickness	in(m)	,
E	= modulus of elasticity	psi(Pa)	,
ν	= Poisson ratio	Dimensionless	,
D	= flexural rigidity=$Eh^3/12(1-\nu^2)$		,
p_0	= center load	psi(Pa)	,
k	= elastic foundation constant	$lbf/in^3(nt/m^3)$	,
m,n	= integers	Dimensionless	

The maximum bending stress at the bottom of an infinite size plate of similar interior load of Figure 11 may be determined from the well known Westergaard equation given in Reference 7 as

$$\sigma_{max} = \frac{.275P}{h^2} \log_{10}\left(\frac{Eh^3}{kR^4}\right) \qquad (6)$$

$$R \begin{cases} = \sqrt{1.6r^2+h^2} - .675h, & r < 1.724h \\ = r, & r > 1.724h \end{cases}$$

where, in addition to the symbols above

P	= $p_0 \pi r^2$ total load	lb(nt)	,
r	= radius of loaded area	in(m)	.

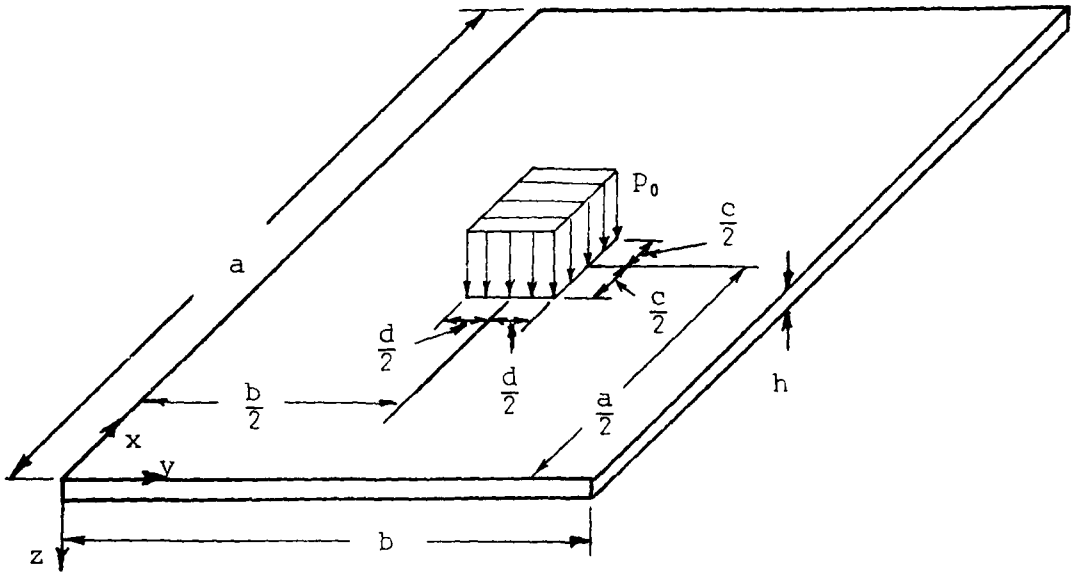

Figure 11. Schematic of Centrally Loaded Plate.

This equation is based on regular plate theory for r greater than 1.724h. However, for r less than 1.724h, thick plate theory was used, which takes into account stresses normal to the plate and the three dimensional nature of the problem.

For both the finite plate, Equation (5), and the infinite plate, Equation (6), caution must be used in selecting a plate size for a given stress. Both equations exhibit a maximum point as shown for a case of the Westergaard equation in Figure 12. This maximum point closely approximates the separation boundary between regular plate theory from the flexible plate theory where combined bending and membrane loads must be considered. For all analysis shown in this report care was taken to insure that thicknesses and related stresses fall to the right of this maximum. This maximum point can be readily determined for the Westergaard equation by simply differentiating Equation (6) partially with respect to plate thickness h and setting the result to zero. However, for the finite plate, Equation (5), the maximum must be found by numerical solution over a wide range of thicknesses.

A general solution to Equation (5) would be to divide the left hand side by the term outside the summation of the right hand side and solve the dimensionless results for various values of m, n, and

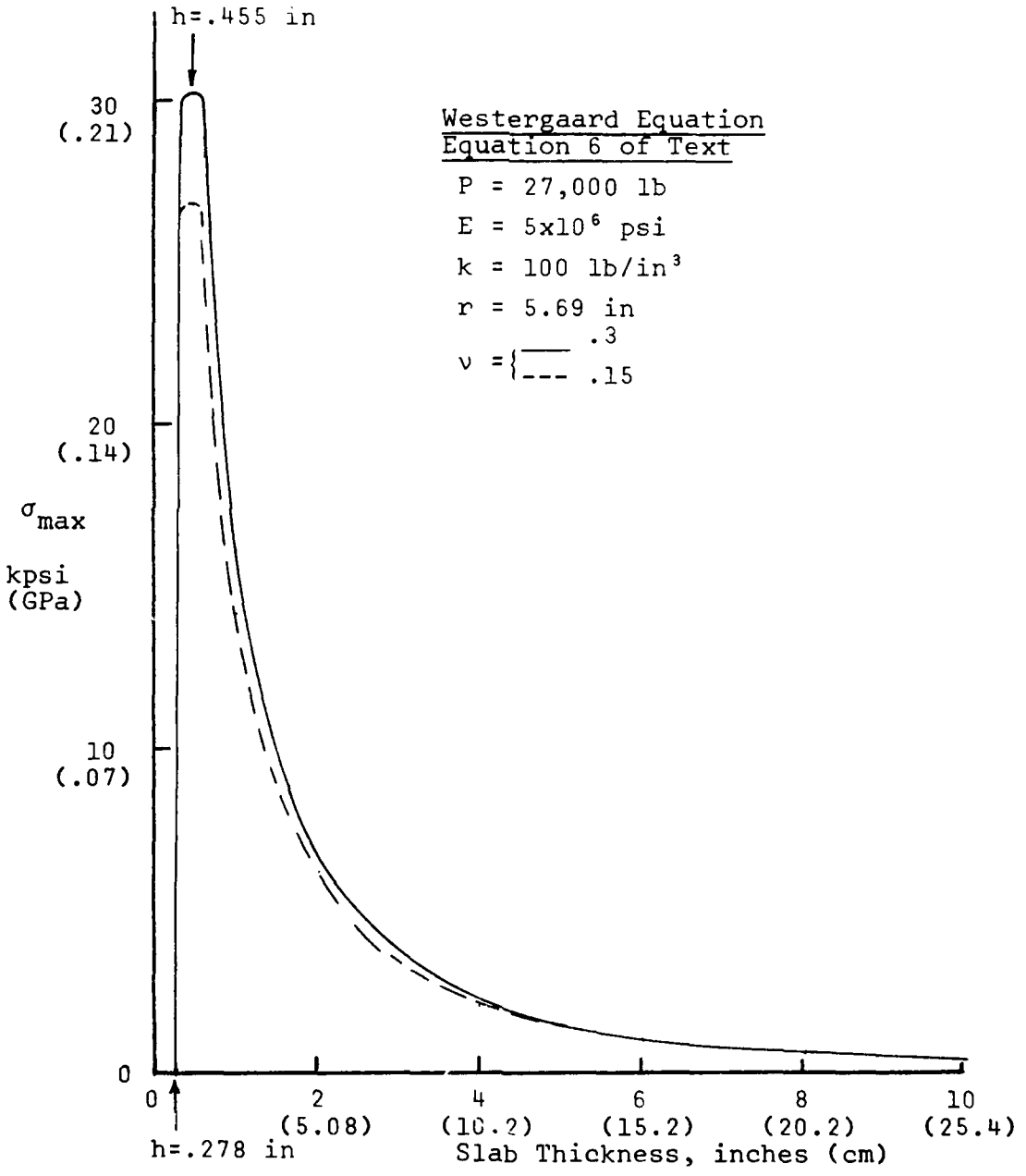

Figure 12. Westergaard Equation for Interior Load.

a^4k/D. This general solution is shown in Figure 13 for $\nu = 0.3$, $a = 240$ inches and various values of a/b. Equation (5) is non-zero only for odd values of m and n and a check on convergence showed that a summation for $m = n = 499$ was sufficient for convergence but in most all cases the summation for $m = n = 999$ was used.

2. POLYMER CONCRETE REPAIR

From the standpoint of material selection for repair, concrete and/or asphalt would probably be the logical choice for runway repair but curing time for both of these materials is just too long. In recent years polymer concrete has been developed and has shown some promise as a fast curing material for rapid runway repair. In an effort to determine minimum thickness required for a concrete repair, Equation (5) has been solved for various values of a, a/b, h and two values of k. Figures 14 through 16 are given for $k = 100$ lb/in^3 (0.27 Gnt/m^3) and Figures 17 and 18 are given for $k = 1000$ lb/in^3 (2.7 Gnt/m^3). For each of the calculations the central load $p_0 = 265$ psi (1.14 MPa), Poisson ratio $\nu = 0.15$ and the modulus of elasticity $E = 5 \times 10^6$ psi (34.5 GPa). Although the maximum stress will occur when the load is at the plate center the problem arises that the aircraft must pass over the plate edge to get to the center. For thin plates, the edge stresses could become a problem when the aircraft is close to the edge of the repair. For repairs where the required concrete thickness is relatively thin, a thicker outer edge should be cast to prevent edge cracking under load. Magnitudes of the stress level for edge loads of an infinite plate may be approximated by a Westergaard edge equation given in Reference 2 and discussed in some detail in Reference 5.

3. METAL FOD COVERS

In an effort to reduce failure of the cover material under the wheel loads an aluminum cover was analyzed. An analysis of braking or inplane load was accomplished in a manner similar to that of the T17 material (Figure 8) except that the full plate was used in the analysis. The loading was applied in the same manner, i.e., 100 pounds (445 nt) distributed around the center of the plate. The results of this analysis are shown in Figure 19. In this figure only a quarter of the plate is shown and the right hand lower quarter of the plate would be exactly as the left hand quarter shown. The upper portion has been omitted but the tensile stresses as shown in Figure 19 simply become compressive stresses with the same distribution. This means that the lower portion (behind the load) has principally a tensile stress distribution and the upper portion (ahead of the load) would have a compression

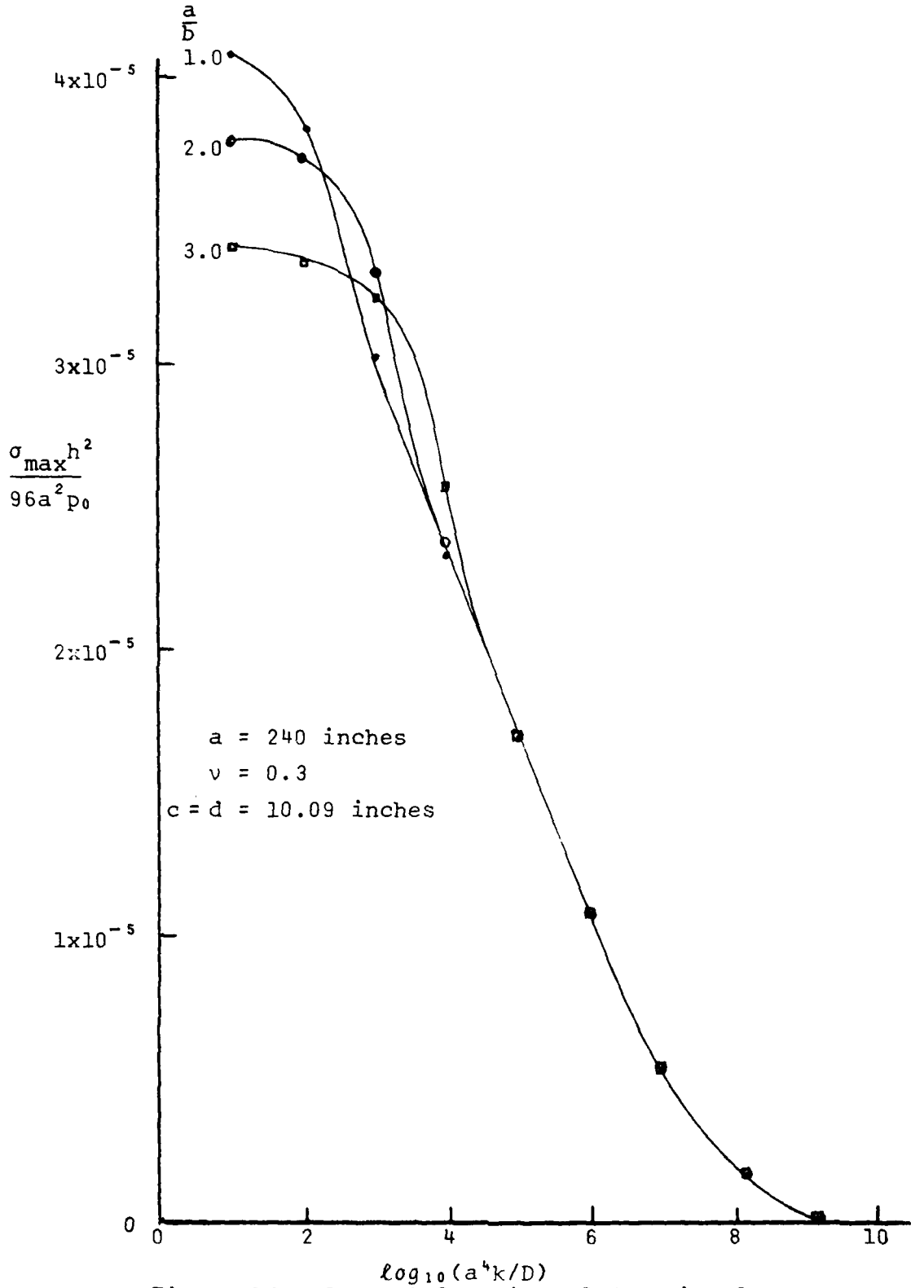

Figure 13. General Solution of Equation 5.

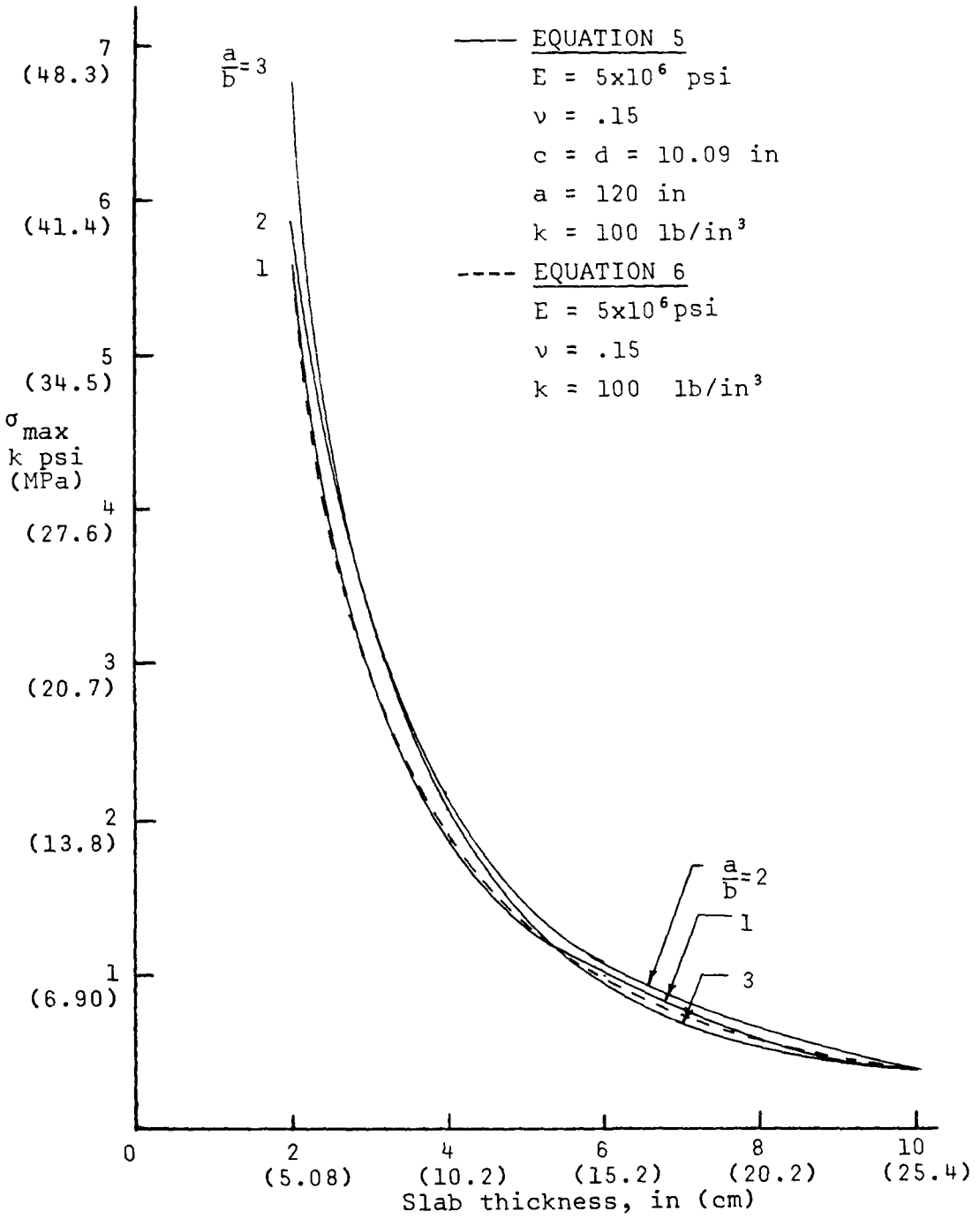

Figure 14. Maximum Bending Stress for Concrete Plate. $k = 100$ lb/in^3, $a = 120$ inches.

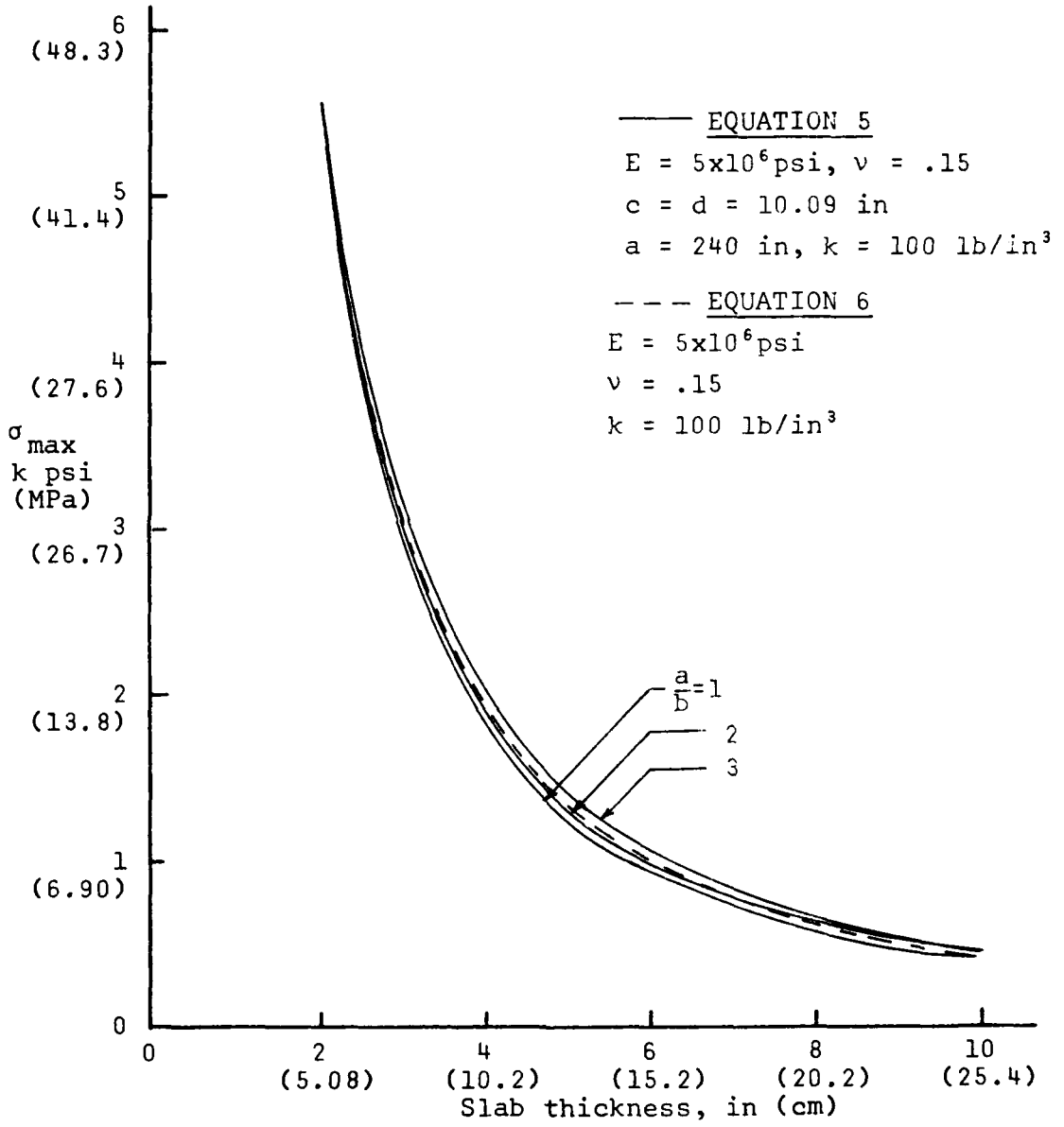

Figure 15. Maximum Bending Stress for a Concrete Plate. $k = 100$ lb/in^3, $a = 240$ inches.

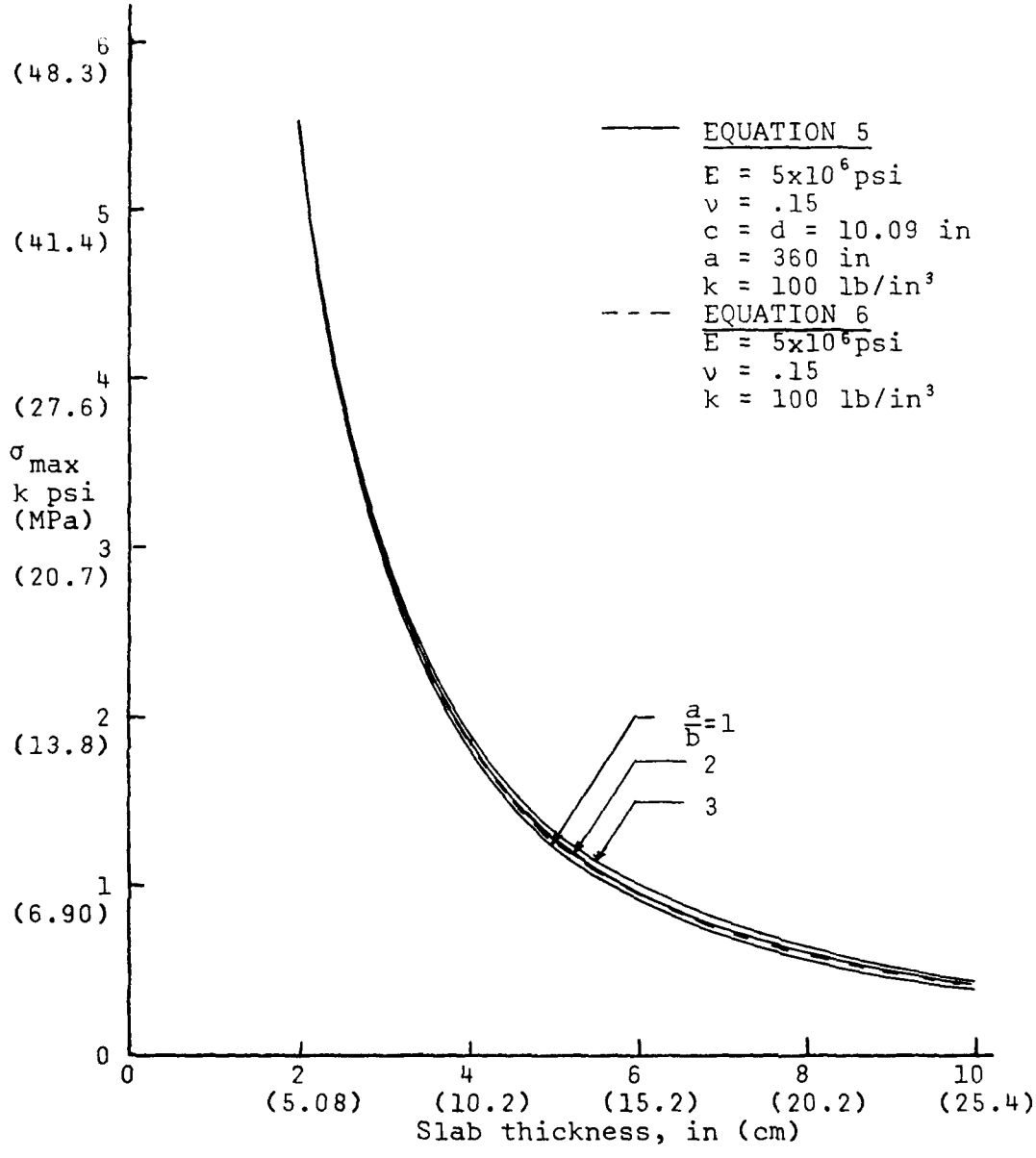

Figure 16. Maximum Bending Stress for Concrete Plate. $k = 100$ lb/in^3, $a = 360$ inches.

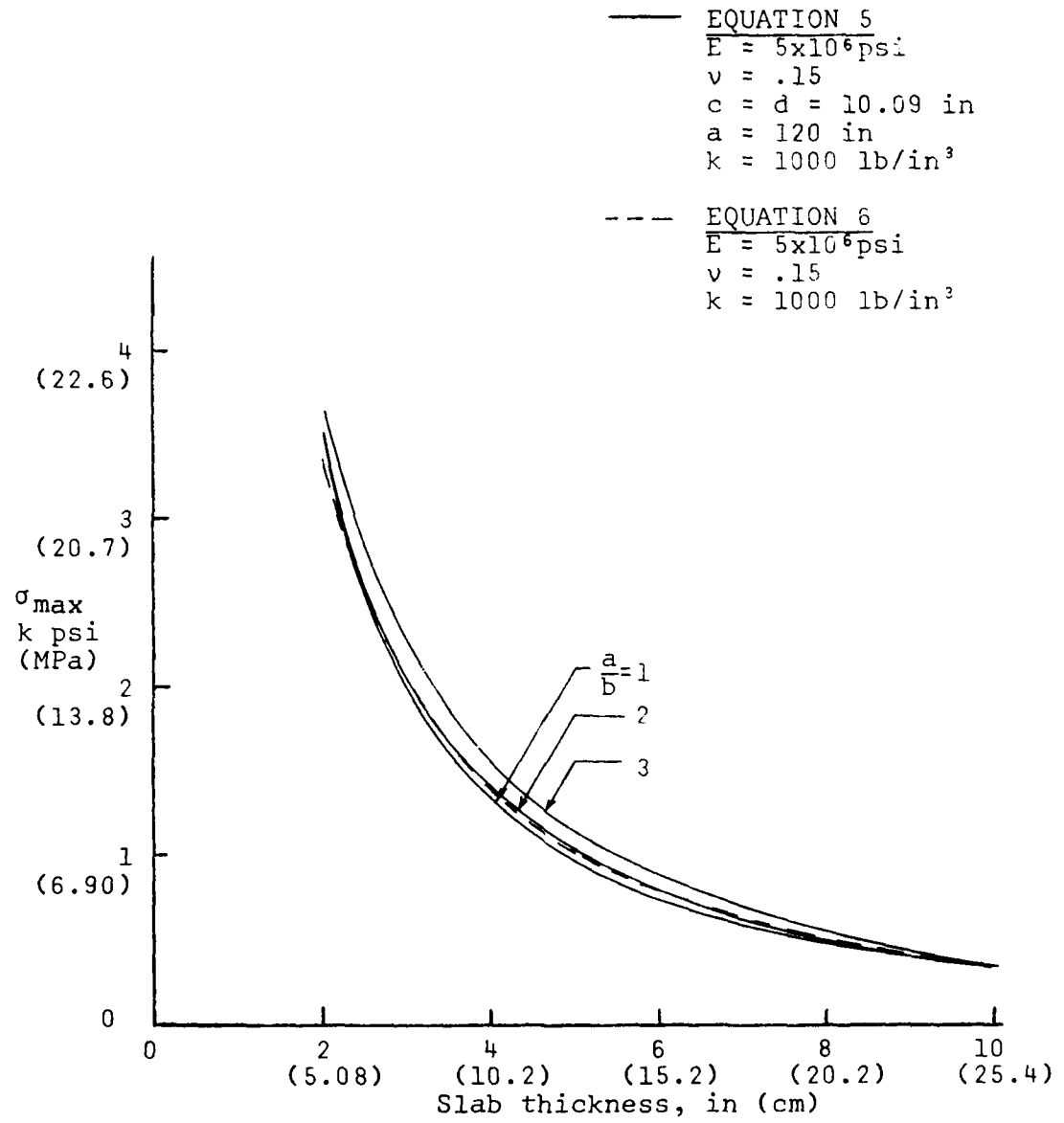

Figure 17. Maximum Bending Stress for Concrete Plate. $k = 1000$ lb/in^3, $a = 120$ inches.

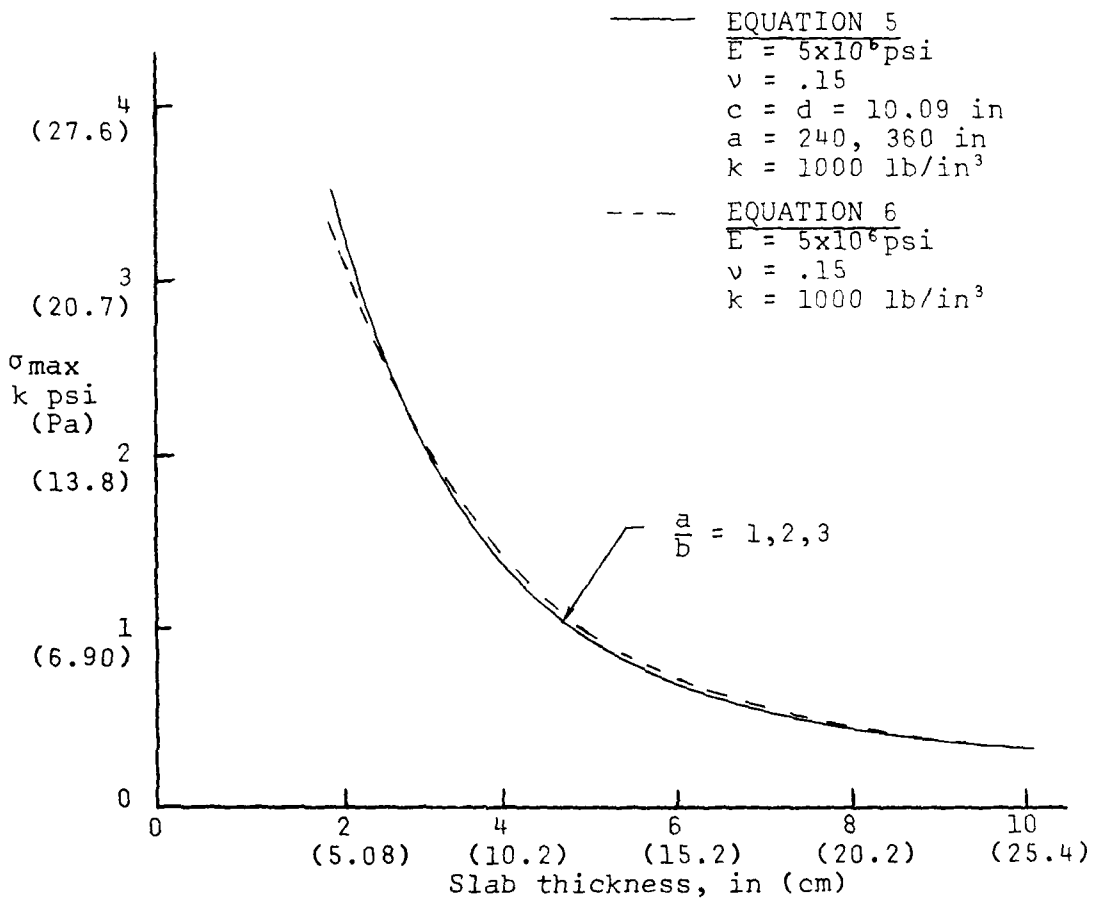

Figure 18. Maximum Bending Stress for a Concrete Plate. $k = 1000$ lb/in^3, $a = 240, 360$ inches.

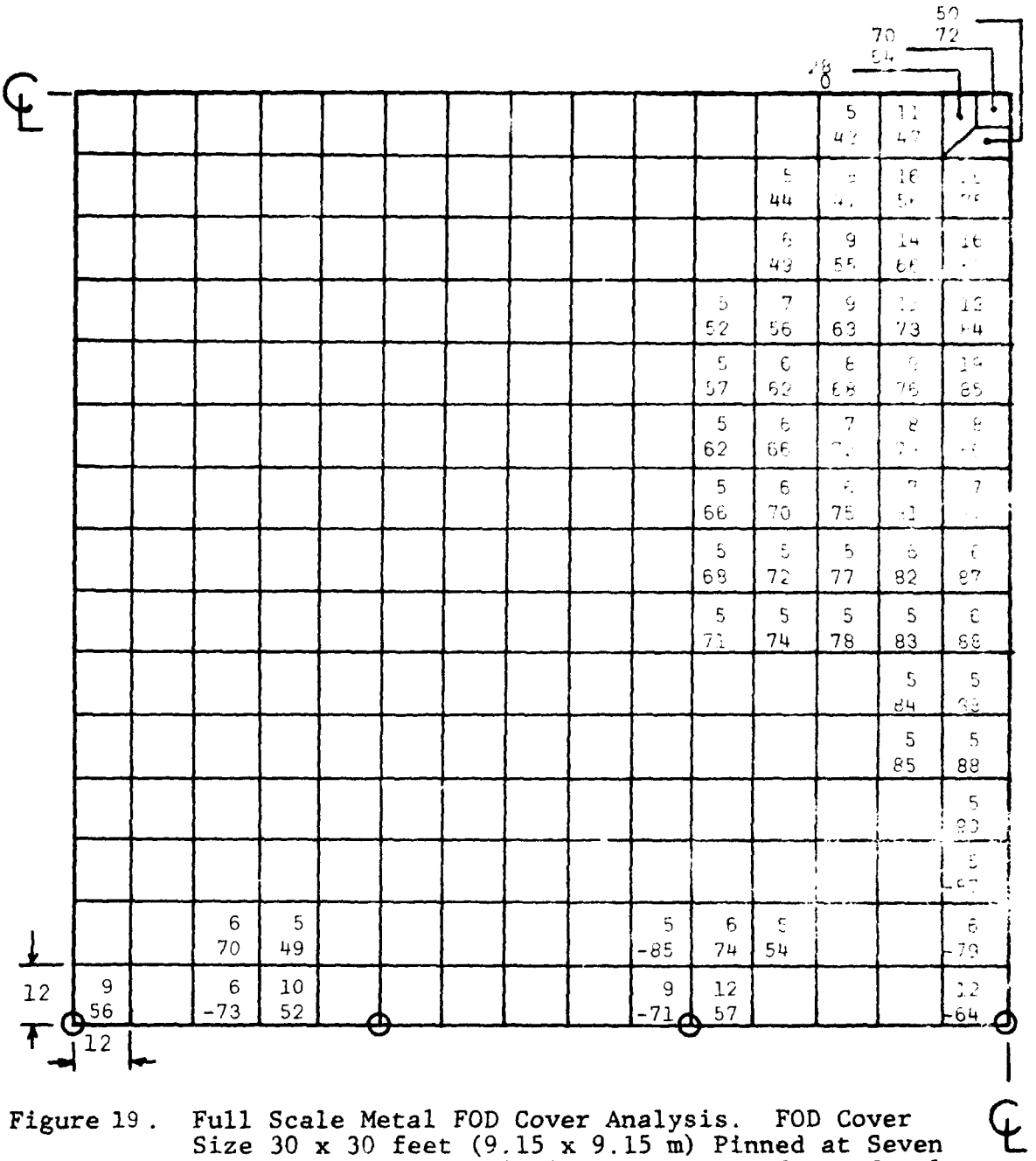

Figure 19. Full Scale Metal FOD Cover Analysis. FOD Cover Size 30 x 30 feet (9.15 x 9.15 m) Pinned at Seven Places as Shown by Circles at Lower Nodes. Total Load on 100 Pounds (445 nt) Distributed at Center of Cover Similar to That of Figure 2. All Stresses Less Than 5 psi are Omitted. Upper Number Denotes Stresses in psi and Lower Number Denotes Principal Direction in Degrees Measured from Line Parallel to Pinned Node Line. Aluminum Material 0.05-inch (0.13 cm) Thick.

distribution equal but opposite to the tensile distribution. The analysis was made for a 0.05-inch (0.13 cm) thick plate and even though the metal material is much stiffer than the flexible T17 material the critical buckling stress for the metal material is very low. This means that for very thin aluminum materials (< 0.1 inch (0.25 cm)) the critical elastic buckling stress is less than 600 psi (4.14 MPa) and upon application of the braking load the material in front of the load will buckle and the major portion of the load will be carried by the plate behind the load. Therefore, for the inplane braking, the only advantage gained by using metal material for a FOD cover is that the failure strength will be increased.

As a check on the bending stress for a metal plate the same general analysis as used for concrete was also used for an aluminum plate. Using Equation (5), with $\nu = 0.3$, $E = 10 \times 10^6$ psi (69 GPa), $p_0 = 265$ psi (1.14 MPa) and with two values of k, 100 and 1000 lb/in^3 (.27 and 2.7 Gnt/m^3), bending stress for the center of a simply supported plate were determined for various values of a and a/b. The results of these analyses are given in Figures 20 through 22. For $k = 1000$ lb/in^3 and plate sizes considered the results appear to be independent of plate size and a/b ratio. This is confirmed by results of Figure 13 where the solution at large values of a^4k/D is independent of a/b ratio. As one might suspect the thickness required to reduce the bending stress level below 30,000 psi (172.4 MPa), an acceptable tensile yield stress in wrought aluminum sheet, is exceptionally high. The basic reason for such large thickness lies in the fact that bending stress for plates without elastic foundations will be independent of the plate material and solely dependent on plate dimensions and boundary conditions. The inclusion of the foundation k requires inclusion of the flexural rigidity D for the plate. This same kind of phenomenon occurs in metal beams and shafts and of course the methods used to reduce the large thicknesses for these cases are to use hollow shafts, thin vertical web beams and composite plates with low strength filler or stiffening material. The metal plate problem was encountered in the development of the AM-2 mat where an overall thickness of 1.5 inches (3.81 cm) was used with stiffeners placed between two reasonably thin aluminum plates. This is not to say that metal plates are to be avoided but thin plate analysis, which takes into account stretching of the plate midplane and flexibility of thin plates, must be exercised. This problem is much more complicated than the solutions previously presented for the reasonably thick concrete plates.

4. FLEXIBLE FOD COVER TIE DOWNS

One of the disadvantages of the flexible FOD covers as used is that jet or propeller blast can get underneath the cover and

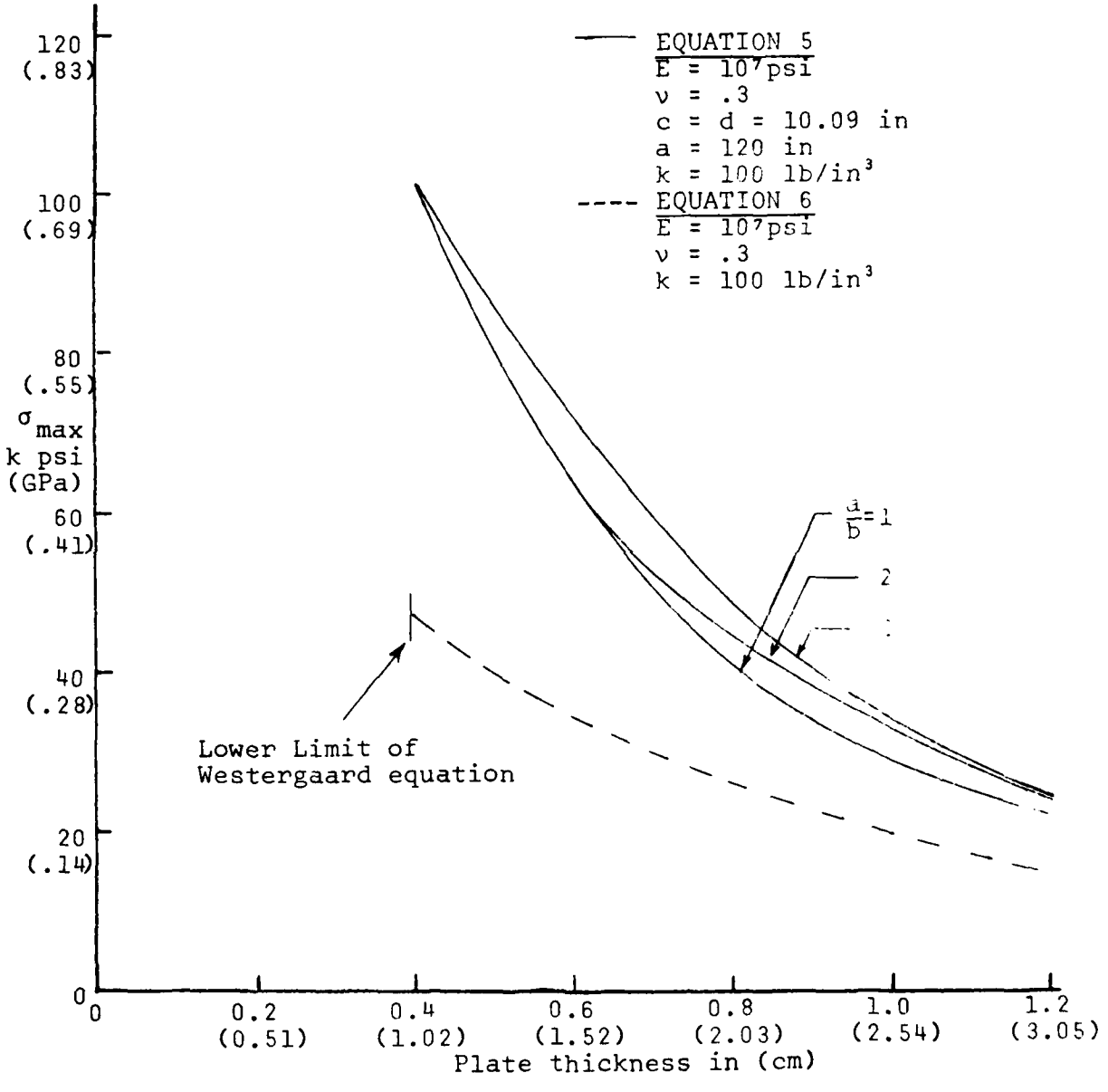

Figure 20. Maximum Bending Stress for an Aluminum Plate. $k = 100$ lb/in^3, $a = 120$ inches.

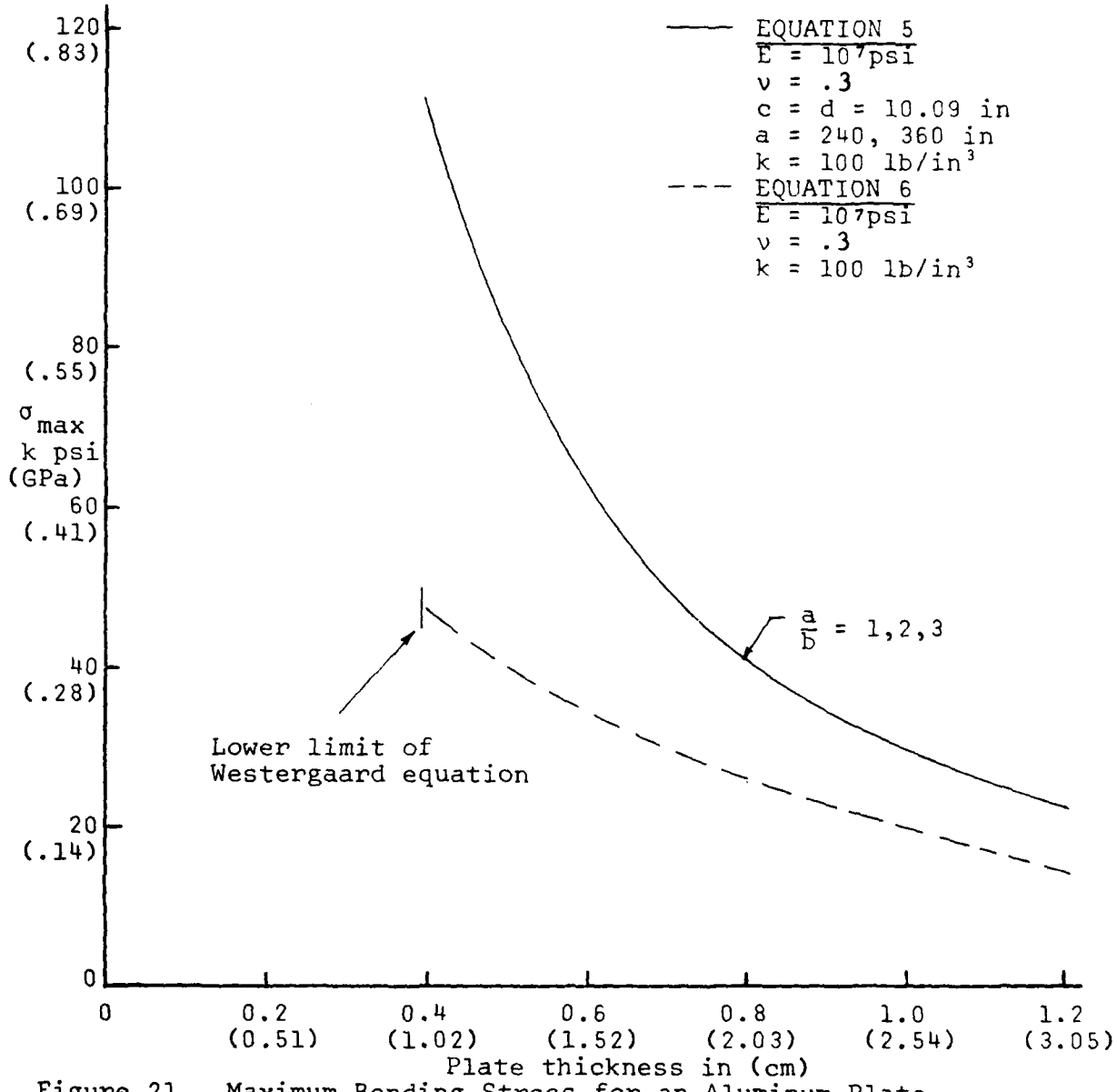

Figure 21. Maximum Bending Stress for an Aluminum Plate. $k = 100$ lb/in^3, $a = 240$, 360 inches.

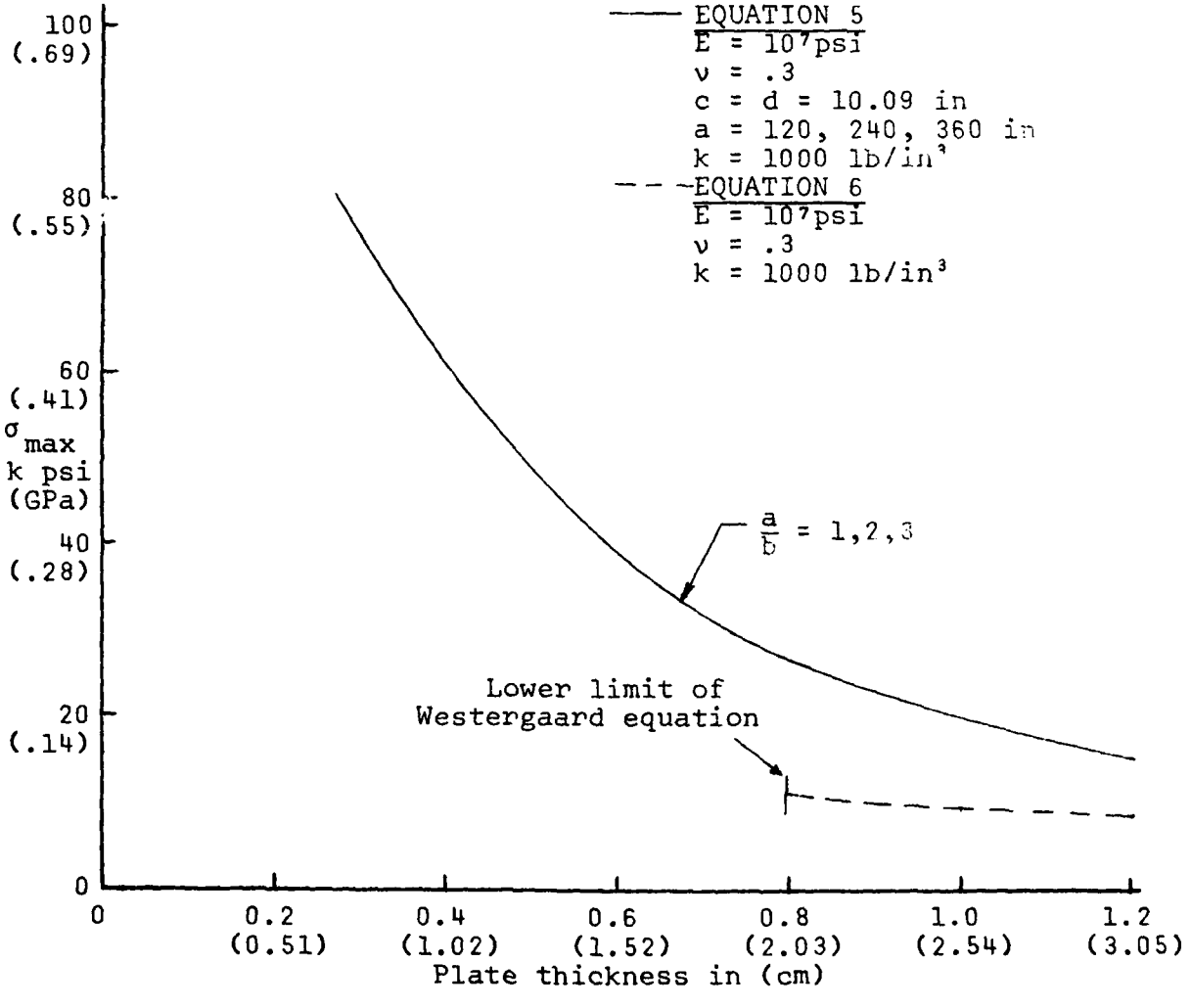

Figure 22. Maximum Bending Stress for an Aluminum Plate. $k = 1000$ lb/in^3, $a = 120, 240, 360$ inches.

cause lifting of the cover thus imposing additional membrane stresses in the cover. The pinning of the sides could eliminate this problem, however this would give increased time for initial installation and subsequent removal and repair if required. Increased stability of the sides of the flexible FOD cover could be obtained by a taut cable attached to the sides of the cover and tied to the pinned ends. The cable could be installed very quickly along with the proper installation procedure. The following discussion describes one cable installation procedure.

If the size of the cover is chosen as X of Figure 23a then the pinned-end length could be extended 6 inches (15.24 cm) on either side as shown in Figure 23a. After the pinned-end X has been pinned down and cables attached at pins marked A the cover is pulled out in the opposite direction of the repaired crater. With the cover under side up the cables are laid down and the flaps folded over and contact cemented to the exposed under side of the cover as shown in Figure 23b. After the crater is repaired the cover is then pulled over the crater and the Y-end pinned to the runway. The loose cable ends are then pulled taut and fixed at pins marked B of Figure 23c.

It is expected that a 0.125-inch (0.318 cm) diameter aircraft cable with 100-200 lbf (445-890 nt) tension would be sufficient to hold down the loose edges of the flexible FOD cover.

5. PHASE II DISCUSSION, CONCLUSIONS AND RECOMMENDATIONS

It is concluded that some type polymer concrete would be the logical material for rapid repair if all the problems associated with handling, mixing, cure time, and shrinkage, shelf life, etc. could be eliminated. However, with increased strength and associated decrease in thickness required for the given load, the problem of excessive deflection must be considered. This problem has been ignored in the analyses presented herein. Also decreased thickness and a shift toward resulting membrane stresses complicate the analysis and simple closed form solutions are not available. In addition simple quasi-static material properties may not be sufficient to describe the thinner plate response.

Metal FOD covers offer the advantage of strength but permanent deformation resulting in buckles and wheel ruts will be a problem. Small scale testing of standard metal sheets subjected to typical aircraft loads should be attempted before any full scale test is attempted. Joining problems associated with large thin sheets will almost prohibit their use.

Thin flexible membranes lend themselves very well to ease of handling and rapid repair. If continued use of the flexible

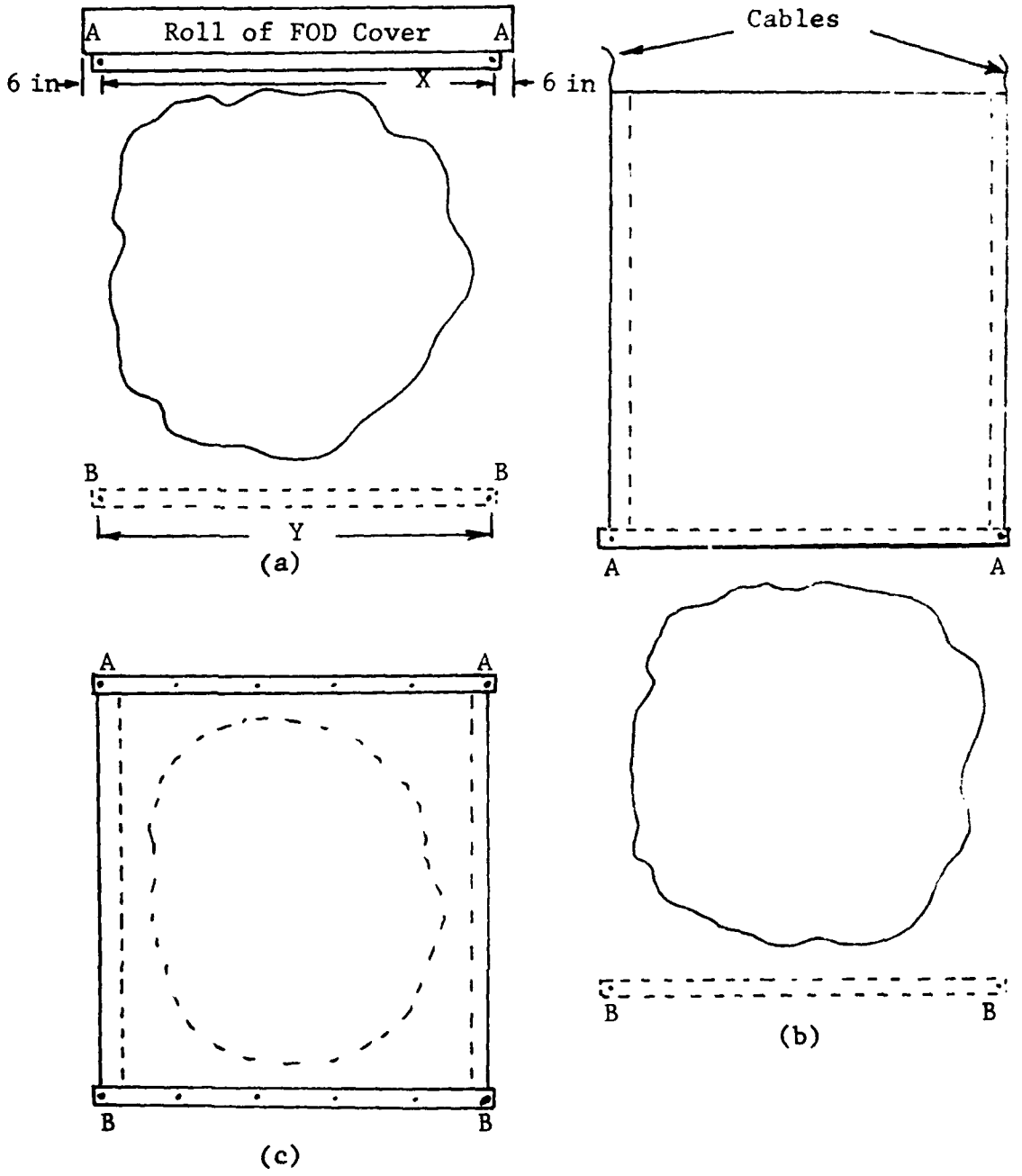

Figure 23. Schematic of Cable Tie Down of FOD Cover Sides.

membrane is dictated then studies into stronger filaments or a hybrid system of cloth-metal fibers or glass-metal fibers bound by a flexible matrix would be recommended. The T17 material with reinforced 0.063-inch (0.159 cm) cables on a 4.0-inch (10.16 cm) grid or just running parallel with take-off direction could prove capable of carrying the braking loads. In all cases of flexible covers it is recommended that all edges be held down in some manner.

REFERENCES

1. Vollor, T. W., "Comparison of Performance of Experimental Membranes, Nonskid Compounds, Adhesives, and Earth Anchors with Regard to C-130 Aircraft Operational Requirements," WES-TR-S-71-11, U. S. Army Waterways Experiment Station, Vicksburg, Mississippi.

2. Timoshenko, S., and Woinowsky-Krieger, S., Theory of Plates and Shells, McGraw-Hill Book Co., 1959.

3. Szilard, R., Theory and Analysis of Plates, Classical and Numerical Methods, Prentice-Hall, Inc., 1974.

4. Hughes, W. F., and Brighton, J. A., Theory and Problems of Fluid Dynamics, Schaum's Outline Series, Schaum Publishing Co., 1967.

5. Yoder, E. J., and Witczak, M. W., Principles of Pavement Design, 2nd Ed., Wiley Interscience Pub., John Wiley & Sons, New York.

INITIAL DISTRIBUTION

DDC-DDA-2	12
HQ AFSC/DLWM/SDNE/DEE/DEM	4
HQ USAFE/DEMY/DEM/DEX	3
HQ USAFE/EUROPS (DEXD)	1
AFATL/DLJK/DLODL	2
AD/IN	1
USAFTAWC/RX/THL/THLA	3
EOARD/LNS	1
SHAPE Tech Center	1
HQ PACAF/DEE/DEMM/DEM/DEPR	4
HQ TAC/DEE/DRP	2
AUL/LSE 71-249	1
COMMCBLANT	1
AFISC/IGQB	1
HQ SAC/DE/DEE/DEM	3
US Navy Civil Engrg Lab	1
HQ ATC/DED/DEE	2
HQ MAC/DEM	1
HQ AFESC/DEMP/DEO/TST	3
HQ AFESC/RDCR	5
BDM Corp	2
USAE WESGF	1
HQ USAF/LEEX/LEYW/RDPX	2
AFWAL/MMXE/FIEM/FIBE	3
HQ AFLC/DEMB/DEE	2
AFIT/DET/LDE	2
ASD/TAAMF	1
819 CESHR	1
200 CESHR/CC	1
201 CESHR/CC	1
Det 1, 307 CESHR/CC	1
307 CESHR/CC	1
554 CESHR/CC	1
Det 1, 554 DESHR/CC	1
820 CESHR/CC	1
823 CESHR/CC	1
HQ AAFCE	1
TAC ZEIST	1
559 CE CFE HQ	1
HQ 3 in C, Moduk (Army)	1
Luftwaffenpionierlehr Kompanie	1
LuftflottenKommando A3V	1
Etat-Major	1
Etat-Major Force Aerienne	1
Fixed Wg Eng Tech Sec, A&Aee	1
Defense Equip. Staff Brit Emb.	1
Procurement Exec. Min of Def.	1
Dept of Civil Engrg, Mar. Univ.	1
Univ. of Florida, Grad Engrg Cen	5

(The reverse of this page is blank.)


DATE
ILME